

Dissertationes Forestales 349

Novel methods facilitating the mechanistic interpretation
of multiscale optical remote sensing measurements

Jaakko Oivukkamäki

Institute for Atmospheric and Earth System Research / Forest Sciences

Department of Forest Sciences

Faculty of Agriculture and Forestry

University of Helsinki

Finland

Academic dissertation

To be presented, with the permission of the Faculty of Agriculture and Forestry of the University of Helsinki, for public examination in lecture room 2402, Biocenter 3-building (Viikki Campus, Viikinkaari 1, Helsinki) on the 1st of February 2024 at 12 o'clock.

Title of dissertation: Novel methods facilitating the mechanistic interpretation of multiscale optical remote sensing measurements

Author: Jaakko Oivukkamäki

Dissertationes Forestales 349

<https://doi.org/10.14214/df.349>

© Author

Licensed [CC BY-NC-ND 4.0](https://creativecommons.org/licenses/by-nc-nd/4.0/)

Thesis supervisors:

Professor Albert Porcar-Castell

Institute for Atmospheric and Earth System Research (INAR)/Forest Sciences

Department of Forest Sciences, University of Helsinki, Finland

Docent Jon Atherton

Institute for Atmospheric and Earth System Research (INAR)/Forest Sciences

Department of Forest Sciences, University of Helsinki, Finland

Pre-examiners:

Senior Researcher José Javier Peguero Pina

Agrifood Research and Technology Centre of Aragón (CITA), Spain

Professor María Gabriela Lagorio

University of Buenos Aires, Faculty of Exact and Natural Sciences, Argentina

Opponent:

Research Manager Markku Keinänen

Faculty of Science, Forestry and Technology, University of Eastern Finland, Finland

ISSN 1795-7389 (online)

ISBN 978-951-651-788-2 (pdf)

Publishers:

Finnish Society of Forest Science

Faculty of Agriculture and Forestry of the University of Helsinki

School of Forest Sciences of the University of Eastern Finland

Editorial Office:

Finnish Society of Forest Sciences

Viihinkaari 6, 00790 Helsinki, Finland

<https://www.dissertationesforestales.fi/>

Oivukkamäki J. (2024). Novel methods facilitating the mechanistic interpretation of multiscale optical remote sensing measurements. *Dissertationes Forestales* 349, 69 p. <https://doi.org/10.14214/df.349>

ABSTRACT

Plant physiology concentrates on the study of plant internal processes, such as growth, nutrient uptake and photosynthesis. The quantification of photosynthesis regulation is significant in understanding how plants react to the changing climate. Spectral remote sensing methods, using both reflected light in the visible and near infrared wavelengths, as well as chlorophyll fluorescence, are used to gather information about plant physiological variables. These methods have developed rapidly, prompted by the advances in remote sensing platforms and sensors.

However, interpretation of remote sensing signals can be challenging. Due to canopy heterogeneity, the signal is affected by various elements, such as scattering, soil background and canopy structural effects. Additionally, open questions remain linked to the underlying mechanistic processes in the leaf modulating the optical signal, such as nutrient contents and leaf photochemistry, and how these processes and the optical signals diverge in response to temporal variation. Through multi-scale measurements, this thesis aims to advance the interpretation of optical remote sensing signals as they are affected by spatial and temporal variation, while promoting the use of novel methods and devices.

Results indicate that diurnal and long-term variation of solar induced fluorescence (SIF) is driven by photosynthetic and structural factors, causing possible misinterpretations in SIF data. Additionally, depending on the scale of observation, results show that the capacity of remote sensing to detect changes in foliar nutrients depends on the covariation of nutrients, pigments and canopy structure, underlining the need for both leaf and canopy level measurements. Finally, we advocate for the implementation of a novel miniaturized fluorometer, demonstrating the ability to track the seasonal regulation of photosynthesis using integrated measurements of chlorophyll fluorescence and gas exchange. The results from this thesis underline the need for simultaneous multi-scale measurements of leaf and canopy physiological factors to further our understanding of photosynthesis regulation.

Keywords: Chlorophyll fluorescence, vegetation indices, photosynthesis, nutrients, carbon assimilation, multi-scale measurements

TIIVISTELMÄ

Kasvien fysiologian tutkimus keskittyy kasvin sisäisten prosessien, kuten kasvun, ravinteidenottokyvyn ja fotosynteesin tutkimiseen. Fotosynteesin säätelyn mittaaminen on merkittävää ymmärtääksenne, miten kasvit reagoivat muuttuvaan ilmastoon. Valon spektriin perustuvia kaukokartoitusmenetelmiä, jotka käyttävät näkyvää ja lähi-infrapuna-aallonpituuksilla heijastunutta valoa, sekä klorofyllifluoresenssia, käytetään keräämään tietoa kasvin fysiologisista muuttujista. Nämä menetelmät ovat kehittyneet nopeasti kaukokartoituslaitosten ja sensoreiden kehityksen myötä.

Kaukokartoitustulosten tulkitseminen voi kuitenkin olla haasteellista. Latvuston heterogeenisuuden vuoksi mittaussignaaliin vaikuttavat erilaiset tekijät, kuten ilmacehästä johtuva hajonta, mitattavan kasvuston tausta ja kasvuston rakenteelliset ominaisuudet. Lisäksi optiseen kaukokartoitussignaaliin vaikuttavat lehden fysiologiset prosessit, kuten lehden ravinnetasapaino ja lehden valokemia, sekä miten nämä prosessit ja optiset signaalit muuttuvat ajallisen vaihtelun seurauksena. Tämän väitöskirjan tavoitteena on edistää optisen kaukokartoituksen signaalitulkintaa, edistäen samalla uusien menetelmien ja laitteiden käyttöönottoa.

Tulokset osoittavat, että aurinkoinduktiivisen fluoresenssin (SIF) päivittäinen ja pitkäaikainen vaihtelu latvustossa johtuu sekä fotosynteesistä ja rakenteellisista tekijöistä, mikä saattaa aiheuttaa virheellisiä tulkintoja SIF-mittauksista. Lisäksi tulokset osoittavat, että kaukokartoituksen kyky havaita muutoksia lehtiravinteissa riippuu ravinteiden, pigmenttien ja kasvustorakenteen yhteisesiintymisestä, korostaen samanaikaisten lehti ja latvustotason mittausten tärkeyttä. Esittelemme myös uudenlaisen miniaturisoidun fluoresenssimittarin, joka demonstroi kyvyn seurata fotosynteesin kausittaista säätelyä klorofyllifluoresenssin ja kaasunvaihdon integroiduilla mittauksilla. Tämän väitöskirjan tulokset korostavat tarvetta samanaikaisille ja monimittakaavaisille lehtien fysiologisten tekijöiden mittauksille, jotta voisimme edistää ymmärrystämme fotosynteesin säätelystä.

ACKNOWLEDGEMENTS

While there is only one name on the cover of this academic dissertation, all the work leading up to it has by no means been an individual effort. I have received help not only from my supervisors and co-authors, but also from the lovely people of the Optics of Photosynthesis laboratory and the Ecosystem processes group, who have generously sacrificed their time to help me. Writing this dissertation was a long and convoluted road which led me to grow both as a researcher and as a human being. It included long days of field work in potato fields and in dark, windowless rooms, but also moments of real innovation and clarity, which made the journey all worth it.

While it was sometimes difficult to keep the faith between innumerable article versions, I sincerely appreciate the positive attitude, help and constructive criticism offered by my supervisors Albert Porcar-Castell and Jon Atherton. Our meetings really made me understand the tenacity and insight needed to become a successful researcher. In addition, I would like to thank Paulina, Chao, Luis, Steffen and Anu, as well as all the other past and present members of the OPL group for their help over the years. Additionally, a special thank you to Teemu P, Angi, Anna and the rest of the Ecosystem processes group, as well as all the co-authors of the articles included in this dissertation. I would also like to thank the staff at the department of forest sciences and at the Hyytiälä Forestry field station (especially Juho Aalto) for their assistance. Finally, I would like to thank the members of my thesis committee for their guidance during this process: Liisa Kulmala and Esa Tyystjärvi. For financial support, I am thankful for the doctoral programme of atmospheric sciences as well as Jaana Bäck for making this research possible.

Lastly, although my mother passed away during my PhD journey, I will always be grateful for the unconditional support offered by my parents, no matter what path I chose in life. In the same way, I want to thank my brother and sister for their support. As a final note, the dedication and care offered by my wife Heidi has been nothing short of extraordinary and I am forever grateful to her, as I am grateful to my children Eero and Aili for reminding me about the important things in life (which may not always be related to plant optical signals). And to anyone reading this struggling with their PhD: you'll get there.

LIST OF ORIGINAL ARTICLES

This thesis consists of a summary part and three original publications. Two original research articles have been published in peer-reviewed journals and the third one is a ready manuscript submitted to a peer-reviewed journal as a methods paper. The articles are hereafter referred to by their Roman numerals.

I Xu, S., Atherton, J., Riikonen, A., Zhang, C., **Oivukkamäki, J.**, MacArthur, A., Honkavaara, E., Hakala, T., Koivumäki, N., Liu., Z. & Porcar-Castell, A. (2021). Structural and photosynthetic dynamics mediate the response of SIF to water stress in a potato crop. *Remote Sensing of Environment*, 263, 112555. doi:10.1016/j.rse.2021.112555

II **Oivukkamäki, J.**, Atherton, J., Xu, S., Riikonen, A., Zhang, C., Hakala, T., Honkavaara, E. & Porcar-Castell, A. (2023). Investigating Foliar Macro-and Micronutrient Variation with Chlorophyll Fluorescence and Reflectance Measurements at the Leaf and Canopy Scales in Potato. *Remote Sensing*, 15(10), 2498. doi:10.3390/rs15102498

III **Oivukkamäki, J.**, Aalto, J., Pfundel, E., Tian, M., Zhang, C., Grebe, S., Salmon, Y., Hölttä, T. & Porcar-Castell., A. (2023). Integrating leaf gas exchange and chlorophyll fluorescence to reveal the long-term regulation of photosynthesis *in situ*. Submitted manuscript. doi:10.1101/2023.11.22.568237 [Preprint]

TABLE OF CONTENTS

1. INTRODUCTION	11
1.1 Plant physiology and Remote Sensing	11
1.2 Reflectance based remote sensing methods	13
1.3 Chlorophyll Fluorescence – theoretical background and optical measurements	18
1.3.1 Spectral- and PAM-fluorescence	19
1.3.2 Solar induced fluorescence	21
1.4 Interpretation of the physiological mechanisms affecting leaf spectral emission	22
1.4.1 ChlF imaging systems aid in the mechanistic understanding of the leaf physiology and ChlF relationship	24
1.5 Spatial variation affecting remote sensing signal interpretation	24
2. AIM OF THE STUDY	26
3. MATERIALS AND METHODS	27
3.1 Study sites and plant materials	27
3.2 Leaf level measurements	28
3.2.1 Leaf optical measurements	28
3.2.2 Foliar pigment, nutrient and leaf area analysis	29
3.2.3 Leaf gas exchange measurements	30
3.3 Canopy level measurements	31
3.3.1 Canopy level optical measurements	31
3.3.2 SIF retrieval and processing	32
3.3.3 Estimation of canopy structural parameters	32
3.3.4 Radiative transfer model	33
4. RESULTS	34
4.1 New methods to connect physiological processes to spectral signals at the leaf level	34
4.2 Variables affecting the scaling of leaf spectral signals from the leaf to the canopy	38
5. DISCUSSION	40
5.1 Co-registration of leaf physiological processes and spectral signals	41
5.2 Impacts of canopy structural effects on the scaling of the remote sensing signal from leaf to canopy	43
6. CONCLUSIONS	46

ABBREVIATIONS

Abs: Absorption of radiation energy by the leaf
 ALA: Average leaf angle
 A_{NET} : Net carbon assimilation
 APAR: Absorbed photosynthetically active radiation
 APAR_g: Absorbed photosynthetically active radiation by the photosynthetic pigments
 ATP: Adenosine triphosphate
 Car/Cab: Carotenoid chlorophyll ratio
 CCI: Chlorophyll – carotenoid index
 ChlF: Chlorophyll-a fluorescence
 DMSO: Dimethyl sulfoxide
 E: Transpiration rate
 E_{PAR} : Irradiance integrated from the PAR region
 ETR: Electron transport rate
 EVI: Enhanced vegetation index
 F_0 : Minimal chlorophyll a fluorescence measured in a dark-adapted leaf after a saturating light pulse
 FCVI: Fluorescence correction vegetation index
 F_M : Maximal chlorophyll a fluorescence measured in a dark-adapted leaf after a saturating light pulse
 F_V/F_M : Maximum quantum yield of primary quinone acceptors (Q_A) reduction, i.e., maximum quantum yield of PSII photochemistry
 F_V : Variable chlorophyll a fluorescence, calculated as a difference between F_M and F_0
 FVC: Fractional vegetation cover
 fAPAR: Fraction of the absorbed photosynthetically active radiation
 f_{esc} : Escape probability of chlorophyll fluorescence in the direction of the sensor
 Fratio: Fluorescence peak ratio
 FSPM: Functional-structural plant model
 FWHM: Full width at half maximum
 F685: Fluorescence emission at 685 nm
 GPP: Gross primary productivity
 g_s : Stomatal conductance
 IR: Infrared
 IRGA: Infrared gas analyzer
 I+: Control plot in the water stress treatment
 I-: Non-irrigated plot in the water stress treatment
 LAD: Leaf angle distribution
 LAI: Leaf area index
 LED: Light emitting diode
 LEDIF: Light emitting diode induced fluorescence
 LIFT: Laser induced fluorescence transient
 LUE: Light use efficiency
 MCARI: Modified Chlorophyll Absorption in Reflective Index
 MTA: Mean tilt angle
 MTCI: MERIS terrestrial chlorophyll index
 NADPH: Nicotinamide adenine diphosphate

NDVI: Normalized difference vegetation index
NIR: Near infrared
NIRv: Near infrared reflectance of vegetation
NPQ: Non-photochemical quenching of the chlorophyll fluorescence signal
N1A1: Fertilization regime with half the typical amount of both nitrogen and general fertilizers
N2A0: Fertilization regime with typical amount of nitrogen fertilizer and no general fertilizer
N2A1: Fertilization regime with typical amount of nitrogen fertilizer and half of the typical amount of general fertilizer
N2A2: Fertilization regime with typical amount of both nitrogen and general fertilizers
PAM: Pulse-Amplitude-Modulated fluorescence
PAR: Photosynthetically active radiation
PRI: Photochemical reflectance index
PQ: Photochemical quenching of the chlorophyll fluorescence signal
PSI: Photosystem I
PSII: Photosystem II
R: Range
RH: Relative humidity
RTM: Radiative transfer model
SAVI: Soil adjusted vegetation index
SCOPE: The soil canopy observation of photosynthesis and energy fluxes – radiative transfer model
SFM: Spectral fitting method
SfM: Structure from Motion - method
SI: Sampling interval
SIF: Solar induced fluorescence
SR: Simple ratio
SVP: Saturated vapour pressure
UAV: Uncrewed aerial vehicle
VI: Vegetation index
VPD: Vapour pressure deficit
Y(II): Effective quantum yield of photochemistry
 α_{II} : Partitioning of energy between PSI and PSII
 ϕ_F : Fluorescence quantum efficiency
 Φ_{F_PSII} : Quantum yield of fluorescence in PSII
 Φ_P : operating quantum yield of photochemistry in PSII

1. INTRODUCTION

1.1 Plant physiology and Remote Sensing

The study of plant physiology refers to the investigation of the internal processes and functions of plants, or as Mohr & Schopfer (2012) refer to it: “*Physiology is the science of regulatory and control processes*”. These regulatory and control processes include, to name a few, photosynthesis, respiration, nutrient uptake, stomatal functions and growth. Furthermore, the study of ecophysiology concentrates on how changes in environmental conditions affect these processes. Research in ecophysiology can vary both in scale and in time, from the molecular level all the way to the ecosystem level, as well as from fractions of a second to years (Prasad, 1996, Larcher, 2003). The study of photosynthesis is of distinct interest because of the inherently important role this metabolic process has for all life on earth. Photosynthesis, which is a key driver in the global carbon cycle, uses carbon dioxide (CO₂) from the atmosphere, consequently converted into glucose using photosynthetically active radiation (PAR) as an energy source. Through nutrient uptake, photosynthesis and carbon sequestration, plant ecophysiology is intricately linked to the climate system via the carbon cycle and feedback processes (Heimann & Reichstein, 2008; Sellers et al, 2018). Advancing our knowledge of how plants respond to environmental changes is essential for quantification and modelling of global photosynthesis and is a vital part in understanding and adapting to the impacts of the changing climate.

Remote sensing is the science of acquiring information from an object from afar. The use of remote sensing is widespread in fields such as geology, meteorology, glaciology, hydrocarbon exploration, as well as plant sciences. During the 20th century, remote sensing of Earth’s surface evolved from the first black and white aerial photographs at the beginning of the century to the vast drone and satellite network of the end of the century. Consequently, this has opened the opportunity for quantifying plant growth and photosynthesis from remote sensing platforms (Tucker et al. 1986; Myneni et al. 2002; Sun et al. 2017; Gu et al. 2019). The spatial information that remote sensing measurements provide allows for relatively affordable, fast and repeatable measurements that can reach locations not accessible to field research. In vegetation research, remote sensing has been used since the 1970’s to measure plant biomass (Rouse et al. 1974; Tucker, 1979), and has since seen a wide variety of uses in plant ecophysiology research, such as stress detection and photosynthesis research (Zarco-Tejada et al. 2012; He et al. 2020; Wang et al. 2022).

The development of new technologies and materials during the 20th century allowed for the proliferation of new kind of devices, such as the uncrewed aerial vehicles (UAVs) widely in use today (Everaerts, 2008; Pajares, 2015). Technology improvements have not only caused changes in the platforms used, but also in sensors. While the Landsat satellites, first launched in 1972, housed sensors capable of measuring in the visible, infrared, and thermal infrared range of the electromagnetic spectrum, the contemporary technology meant that the spatial resolution that was available to sensors ranged from 15 - 60 meters. Current satellites can reach a spatial resolution of < 1 m (Al Suwaidi, 2012) with multispectral sensors and can additionally be equipped with modern hyperspectral sensors. While multispectral sensors measure on a number of discrete spectral bands, positioned in specific parts of the electromagnetic spectrum, such as the visible and near-infrared, hyperspectral sensors capture data in hundreds of narrow and contiguous spectral bands, offering higher spectral

resolution data. While covering a wider portion of the electromagnetic spectrum, which allows for the detection of processes undetectable by multispectral sensors, hyperspectral sensors have the trade-off of a lower spatial resolution when compared to lower spectral resolution sensors (Jia et al. 2020).

Additionally, developments have also been made in the interpretation of the data gathered. Reflectance in the red and near infrared (NIR) regions of the spectrum is affected by vegetation structure and by the absorbance and reflectance of the chlorophyll *a* and *b* pigments in the leaves (Curran, 1989; Peñuelas & Filella, 1998; Gutman et al. 2021). Early remote sensing measurements of plants concentrated on developing vegetation indices (e.g. normalized difference vegetation index, NDVI) based on the differences between these regions (Rouse et al. 1974; Tucker 1979). The difference in reflectance between the red and NIR parts of the spectrum is caused by changes in absorption of photosynthetically active radiation (PAR) by chlorophyll. A wide range of vegetation indices have since been proposed, some of them relying on the same principle as the NDVI (e.g., soil adjusted vegetation index (SAVI) and the enhanced vegetation index (EVI)). Additionally, research has also focused on narrowband (e.g. the photochemical reflectance index, PRI) (Gamon et al. 1992) and hyperspectral vegetation indices concentrating on, for example, water and salinity stress (Hamzeh et al. 2013) and chlorophyll detection (Koh et al. 2022).

Finally, in addition to measuring the light reflected from leaves, it is possible to measure chlorophyll fluorescence (ChlF) i.e., radiation emitted by chlorophyll molecules nanoseconds after being absorbed (Maxwell & Johnson, 2000; Baker, 2008). The use of ChlF allows for the investigation of the dynamics of leaf photochemical processes, such as photosynthetic linear electron transport leading to adenosine triphosphate (ATP) and nicotinamide adenine diphosphate (NADPH) production, making it a versatile tool in evaluating leaf photochemistry and CO₂ assimilation (Genty et al. 1989; Lazár, 2015). Thus, combining ChlF and gas exchange measurements could further our understanding of the long-term regulation of photosynthesis, allowing us to quantify the physiological mechanisms driving the optical signals and offering advances in photosynthesis modelling and remote sensing. The connections between ChlF and photochemical processes can be quantified on the leaf level with the aid of pulse amplitude modulated (PAM) -fluorescence. While PAM-fluorescence measurements are limited to the leaf scale, ChlF can now be measured passively at the canopy scale and beyond using solar induced fluorescence (SIF). Although SIF measurements have been conducted since the 1980's (McFarlane et al. 1980), measurements from remote sensing platforms are quite a recent development (Guanter et al. 2007; Meroni et al. 2009; Rascher et al. 2015). The value of SIF comes from its ability to serve as a proxy to plant photosynthetic activity (Yang et al. 2015; Sun et al. 2017), making it a very valuable tool in plant physiology research.

Despite advances in sensor and platform technologies, two inherent issues pertaining to signal interpretation still persist when relating spectral remote sensing with plant functional information and properties, such as plant nutrient contents and photosynthesis. Firstly, to be able to link plant physiological processes and remote sensing, such as SIF and photosynthesis, we need to be able to quantify the leaf level processes that link ChlF and photosynthesis together. This is done via the characterization of leaf level processes such as the diurnal and seasonal dynamics of photosystem II (PSII) energy partitioning and alternative energy sinks (Porcar-Castell et al. 2021). Quantification of these processes on the diurnal and seasonal scales would require long-term field measurements of photosynthesis regulation using both ChlF and gas exchange. Secondly, open questions still remain on how to relate plant functional information to remote sensing measurements when the signal is

affected by spatial change, e.g. from the leaf to the canopy scale. As it is propagated from the leaf to the canopy, the remote sensing signal is affected by various factors, such as chlorophyll reabsorption, measurement geometry, atmospheric effects, scattering, transmission and absorption of the signal. The variation in these factors is driven by sensor positioning, plant physiological processes, as well as canopy structure. As such, the effect that canopy structure has on the relationship between SIF and gross primary productivity (GPP) in varying canopy conditions still has unresolved issues (Study I, Yang & van der Tol, 2018; Dechant et al. 2020). Similarly, the capabilities of various spectral remote sensing methods to detect a wide range of nutrients remain elusive when scaling the signal from the leaf to the canopy. The use of novel methods based on advances in platform and sensor technologies, such as UAV's together with hyperspectral sensors, can aid resolve these issues and would help in the remote sensing of plant functional information, as well as photosynthesis modelling. The combined effects caused by the scaling and leaf physiological dynamics can work either as couplers, affecting the spectral signal and plant physiological variable in the same way, or decouplers, affecting them both differently, impeding the remote sensing signal interpretation. As such, more research is needed to disentangle the effects of these couplers and decouplers in variable temporal and spatial conditions.

For these reasons, it is imperative to gain more knowledge on the influence of the variable mechanistic and spatial factors affecting the remote sensing – plant physiology relationship. In the context of photosynthesis and climate change research, this thesis provides new insights into the development of novel methods and instrumentation for the quantification of these factors, enhancing our understanding of the relationship between spectral remote sensing and photosynthesis on the canopy scale and beyond.

1.2 Reflectance based remote sensing methods

The non-destructive nature, as well as the versatility provided by spectral vegetation indices make them a popular remote sensing product. The underlying mechanism of remote sensing vegetation indices is the interaction of vegetation with light at different wavelengths. However, the quantitative interpretation of remote sensing information from vegetation is a complex task. When quantifying these interactions, we are able to assess changes, for example, in vegetation biomass (Silleos et al. 2006), Leaf area index (LAI) (Liang et al. 2015) and nutrient contents (Jay et al. 2017), as well as how various stressors affect vegetation (Hamzeh et al. 2013; Ihuoma & Madramootoo, 2019) at various spatial scales. This thesis focuses on techniques and technologies based on the visible and infrared (IR) regions of the electromagnetic spectrum. While other active and passive techniques exist, such as Lidar, Radar and microwave based remote sensing, they are beyond the scope of this thesis. The visible region of the spectrum (400 – 700 nm) can be divided by colors, such as blue, green and red regions, while the infrared region can additionally be divided into near IR (780 – 3000 nm) and thermal IR (3000-10000 nm). Since the light that plants absorb to fuel photosynthesis (PAR) is situated in the visible region, this region is of particular interest to vegetation remote sensing. Similarly, while absorbed to a lesser degree, IR radiation is strongly reflected by plants, since they are unable to utilize the photon energy at wavelengths larger than 700 nm in photosynthesis due to chlorophyll pigments absorbance being very low above 700 nm. Between the red and NIR regions of the spectrum is the so-called red edge region of the spectrum, where a sharp increase in reflectance occurs. This region has been

found to be sensitive to the chlorophyll content of the leaves (Horler et al. 1983, Zarco-Tejada et al. 2002) and has been used in vegetation stress detection (Filella & Peñuelas, 1994). Additionally, previous remote sensing research has found that, for example, the reflectance in the shortwave infrared region (1100 – 2500 nm) is highly affected by plant water contents (Curran, 1989; Peñuelas et al. 1993) and can in addition be used to detect stress caused by nutrient deficiencies (Camino et al. 2018; Féret et al. 2021).

To further understand the principle behind the most commonly used vegetation indices (VI), we must first understand what constitutes the reflectance signal from the leaves. Upon reaching the surface of the leaf, radiation can be either reflected, transmitted or absorbed (Figure 1). The fraction of photosynthetically active radiation (PAR) that is absorbed (fraction of the absorbed PAR, fAPAR) depends on the chlorophyll concentration of the leaf

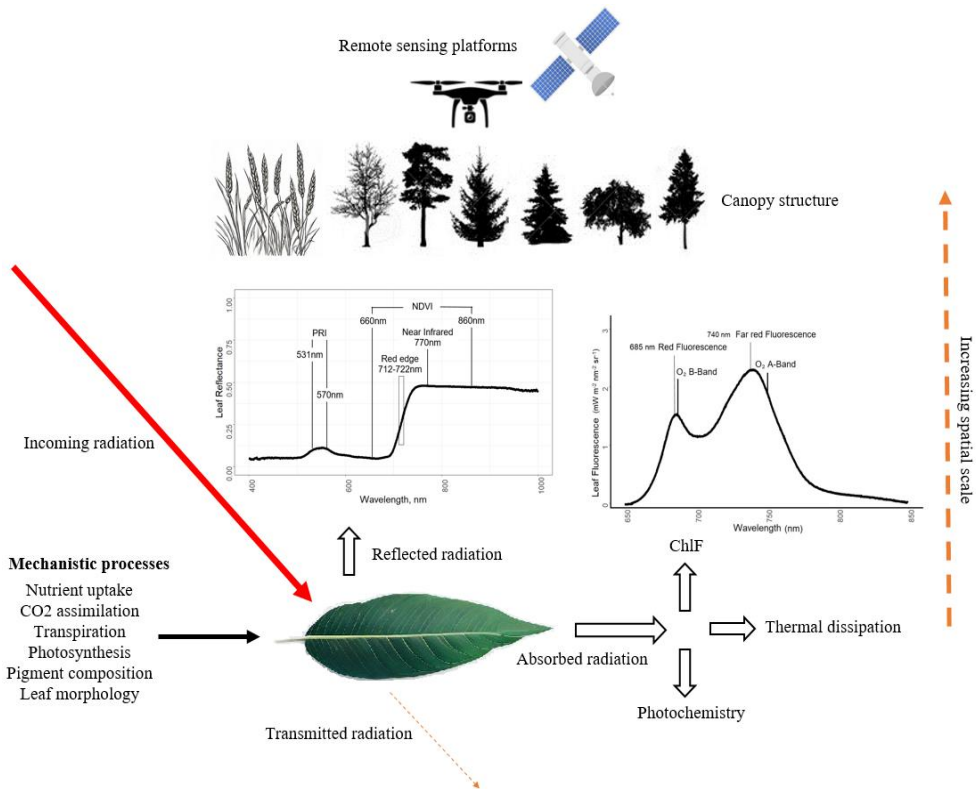


Figure 1 When radiation energy reaches the leaf surface, it can be either reflected, transmitted or absorbed. If reflected, from the spectra of the reflected light, it is possible to calculate vegetation indices detectable by remote sensing instruments. If absorbed, radiation energy has three possible fates: thermal dissipation, use in leaf photochemistry, or re-emission as ChlF. The ChlF spectra has two peaks: the red (~680 nm) and the far-red (~740 nm) peaks. Close to these peaks are the oxygen bands, used often in SIF retrieval. The distribution of reflected, transmitted and absorbed radiation depends on structure and pigment composition of the leaf. When measuring these signals at the canopy scale, the reflected and emitted radiation reaching the sensor on a remote sensing platform is additionally affected by atmospheric scattering and canopy structural properties. Spectra figures adapted from Study II.

(Asner et al. 1998, Peng et al. 2011) as well as a variety of other factors, such as leaf angle (Arena et al. 2008), chloroplast movement (Brugnoli & Björkman, 1992) and anthocyanin concentration (Merzlyak et al. 2008). At the leaf level, the reflectance spectra is primarily affected by the pigment composition (Asner et al. 1998), leaf morphology and additional leaf structural factors (Olascoaga et al. 2014). In turn, the pigment composition depends on several factors, varying seasonally in response to, e.g., environmental stress and nutrient availability (Zhang et al. 2003; Flexas et al. 2004). Four types of pigments make up the pigment composition of a leaf: chlorophylls, carotenoids, anthocyanins and flavonoids. All of these pigments have their own characteristic overlapping absorbance spectra, which together make up the leaf absorbance in the PAR region. Chlorophylls, which are further divided into chlorophyll *a* and *b*, are synthesized in the chloroplasts and are the drivers of photosynthesis in plants (Gates, 2012). Chlorophyll *a* has maximal radiation absorption at 435 nm & 670-680 nm, while for chlorophyll *b* the maximum absorbance is at 392 nm & 626 nm. Furthermore, carotenoids, which play an important role in photosynthesis as well as in protection against photo-oxidative damage (Young, 1991; Dey & Harborne, 1997), absorb radiation highly in the 400 – 500 nm region. Anthocyanins, which have an important function to protect the leaf from photoinhibitory damage (Gitelson et al. 2001), absorb light strongest between 490 nm and 550 nm and flavonoids mainly in the UV-region of the spectrum. Finally, flavonoids typically absorb around the 240-295 nm and 300-380 nm wavelengths and contribute to photosynthesis and play a protective role in plants against biotic and abiotic stressors (Samanta et al., 2011; Taniguchi et al., 2023).

Changes in leaf pigments are driven nutrient availability and stress factors such as drought (Gitelson & Merzlyak, 1994; Flexas et al. 2004; Zhang et al. 2003) as well as by seasonality, best exhibited during leaf development and senescence (García-Plazaola and Becerril, 2001). Drought can cause the plant to close its stomata to conserve water, leading to lower leaf internal CO₂ levels, affecting photosynthesis and chlorophyll production. In the long term, this affects the pigment pools, subsequently mirrored in the reflectance spectra of the plant. Additionally, low water availability has been known to cause the plant to re-allocate nutrients to the top leaves (Yang et al. 2001), which are most often measured in remote sensing measurements (Munné-Bosch & Alegre, 2004), potentially leading to erroneous information about the nutrient status of the plant.

Nutrients are needed by plants to function optimally, and they are divided into micro- and macronutrients, depending on the amount required by the plant. Nitrogen is the most common growth-limiting nutrient and used for vital processes in plants, such as chlorophyll and protein (e.g. RuBisCO) production (Hawkesford et al. 2012). In addition to nitrogen, macronutrients such as phosphorus and magnesium play crucial roles in regulating the photosynthetic process, and their availability can significantly impact a plant's CO₂ assimilation ability (Hawkesford et al. 2012). Furthermore, several micro- and macronutrients are needed for pigment production, such as nitrogen, magnesium and zinc (Natr, 1972). As such, inadequate nutrient availability will harm the pigment production of the plant (Abadía, 1992; Shah et al. 2017), affecting the reflectance and absorbance characteristics. The changes in leaf chlorophyll concentration also alter the absorbance characteristics of the leaf, affecting both reflectance-based remote sensing, as well as ChlF emission. A positive but saturating relationship can be found between leaf chlorophyll concentration and absorbance (Adams et al. 1990, Gitelson et al. 1998) and that of leaf chlorophyll concentration and ChlF emission (Adams et al. 1990).

Vegetation indices are a versatile tool for vegetation remote sensing, and the choice of VI used depends on the specific goals of the analysis, the types of vegetation and environmental

conditions being studied, as well as the characteristics of the remote sensing data available. NDVI, for example, while being widely used, has its disadvantages: saturation in high LAI conditions (Van der Meer et al. 2001; Nguy-Robertson et al. 2012) and sensitivity to soil background noise (Liu & Huete, 1995). While the work of Sellers (1985) showed that NDVI is linearly related to fAPAR, this relationship is tempered by the saturation of NDVI in moderate leaf chlorophyll amounts (Gitelson et al. 1996). As a response to these limitations, additional VI's, such as the Enhanced Vegetation Index (EVI) (Huete et al. 2002) and Soil Adjusted Vegetation Index (SAVI) (Huete, 1988) have been formulated. To answer the need of a growing scientific community measuring a variety of plant species in a wide range of environmental conditions, an expansive list of vegetation indices have been composed. While Table 1 only covers a small part of the VI's in use, it aims to show the multitude of ways that VI's are used in reflectance based vegetation remote sensing and the progress that has been made in remote sensing measurements over the last 70 years. A comprehensive list of significant vegetation indices used in remote sensing of vegetation can be found in the study by Xue & Bu (2017). In this thesis, we used indices such as the photochemical reflectance index (PRI), the chlorophyll – carotenoid index (CCI) and the MERIS terrestrial chlorophyll index (MTCI). Chlorophyll pigments are the main drivers of the reflectance indices based on the red edge region (Horler et al. 1983) and as such, MTCI, calculated using a band in the red edge, has been used for vegetation chlorophyll (Dash & Curran, 2004) and phenology (Boyd et al. 2011) studies, as well as canopy nitrogen level detection on wheat (Bronson et al. 2017) among others. Additionally, vegetation indices can be used to detected canopy structural dynamics, such as the near infrared reflectance of vegetation (NIRv) index, which represents the fraction of NIR originating from vegetation and used in calculating the canopy structural parameter, f_{esc} . Furthermore, and in addition to NIRv, this thesis uses the Fluorescence correction vegetation index (FCVI), which is a reflectance index used to separate the physiological from the non-physiological information in canopy SIF measurements.

Table 1 Reflectance based vegetation indices used in this thesis, as well as commonly used vegetation indices presented together with their formulas and original reference.

Vegetation index	Formula	Reference
NDVI	$\frac{R_{860} - R_{660}}{R_{860} + R_{660}}$	Rouse et al. 1974
SR	$\frac{R_{800}}{R_{670}}$	Jordan, 1969
SAVI	$\frac{(R_{860} - R_{660})}{(R_{860} + R_{660} + L)} + (1 + L)$	Huete, 1988
MCARI	$\frac{1.5 \times [2.5(R_{800} - R_{670}) - 1.3(R_{800} - R_{550})]}{\sqrt{(2R_{800} + 1)^2 - (6R_{800} - 5R_{670}) - 0.5}}$	Haboudane et al. 2004
PRI	$\frac{R_{531} - R_{570}}{R_{531} + R_{570}}$	Gamon et al. 1992
CCI	$\frac{R_{531} - R_{645}}{R_{531} + R_{645}}$	Gamon et al. 2016
MTCI	$\frac{R_{753} - R_{709}}{R_{709} - R_{681}}$	Dash & Curran, 2004

PRI was originally formulated to follow the dynamics of the xanthophyll cycle in plants (Gamon et al. 1992) by measuring reflectance at 531 nm and 570 nm. Reflectance at 531 nm has been found to correlate with the epoxidation state of xanthophyll pigments, involved in the dissipation of excess energy from plants (Adams & Demmig-Adams, 1992) and has been noted to be well correlated with NPQ (non-photochemical quenching, described in section 1.3) in stressed conditions (Evain et al. 2004, Porcar-Castell et al. 2012). This is due to the xanthophyll pigments being associated with diurnal reductions in leaf photosynthetic efficiency as well as increased heat dissipation (Gamon et al. 1992, Panigada et al. 2014). However, the relationship between PRI and NPQ is not straightforward. While short term variation of PRI is linked to changes in NPQ (Porcar-Castell et al. 2012), long term changes in PRI are linked to seasonal changes in carotenoid and chlorophyll pigments (Filella et al. 2009). Additionally, the relationship between PRI and canopy photosynthetic light use efficiency (LUE) has been investigated (Garbulsky et al. 2008). LUE is a parameter often used in photosynthesis modelling, which incorporates environmental and biophysical constraints of the process of converting light energy to plant biomass. While having shown potential as a proxy for LUE (Garbulsky et al. 2008; Middleton et al. 2009), PRI has been shown to be sensitive to canopy structural parameters such as LAI and leaf angle distribution (LAD) (Barton & North, 2001; Goerner et al. 2011), causing the quantification of the relationship to be difficult. Additionally, PRI has been used for nutrient (Peñuelas et al. 1994) and drought stress (Suárez et al. 2009; Zhang et al. 2017) detection. Thus, similarly to ChlF,

PRI offers a deeper understanding of the response of vegetation to changing environmental conditions. The CCI-index, originally developed as an adaptation to PRI to measure photosynthesis dynamics in evergreen forests (Gamon et al. 2016), has been similarly found to be correlated with changes in the xanthophyll cycle.

To summarize, reflectance based vegetation indices can be used to detect changes in plant biomass and leaf area (Silleos et al. 2006; Liang et al. 2015), as well as to quantify the changes to vegetation caused by stress factors such as drought or nutrient limitation (Jay et al. 2017; Ihuoma & Madramootoo, 2019). Additionally, as a part of complementary data inputs, reflectance based vegetation indices can be used to help support SIF interpretation by measuring canopy leaf amounts (Malenovský et al. 2017), related to the to the absorbed PAR by photosynthetic pigments (APAR_g, where g stands for the greenness of the pigments). However, the saturation of spectral reflectance due to canopy structure, as well as susceptibility to background, non-vegetated surfaces affect the retrieved signal. Reflectance based vegetation indices are mainly driven by leaf pigment contents and canopy structural variables and as leaf pigment pools have been found to react relatively slowly to environmental stressors (Song et al. 2018; Chen et al. 2019), these indices might not always be the correct tool for timely detection of stress factors affecting vegetation.

1.3 Chlorophyll Fluorescence – theoretical background and optical measurements

After being absorbed, the radiation energy has three pathways inside the leaf: photosynthesis, thermal dissipation and chlorophyll fluorescence (Butler, 1978). These three pathways are complementary to each other, and as such, the energy used in either photochemistry or thermal dissipation affects the amount of ChlF emitted by the leaf. The energy used in the photochemistry of the leaf is termed photochemical quenching (PQ) of ChlF, while thermal dissipation is named non-photochemical quenching (NPQ) of ChlF. According to the Butler model (Butler, 1978), when NPQ is assumed constant, ChlF allows for the estimation of the photochemistry of the leaf. Research has shown, however, that NPQ is rarely constant, but changes with environmental conditions (Kramer et al. 2004; Porcar-Castell et al. 2014), thus requiring estimation of the quenching mechanisms to investigate the true relationship between ChlF and photosynthesis. At the leaf level, quenching mechanisms can be estimated with the use of pulse amplitude modulated (PAM) fluorescence, helping to resolve the factors affecting the photochemistry of plants (Maxwell & Johnson, 2000).

While most of ChlF originates from photosystem II (PSII), photosystem I (PSI) also contributes to the signal (Farooq et al. 2018). ChlF is emitted from the leaf between the wavelengths of 650 – 850 nm and it has two maximum emission peaks: the red peak at 685 – 690 nm and the far-red peak at 740 – 750 nm (Lichtenthaler & Rinderle, 1988). Leaf pigment composition not only affects the reflectance characteristics of the leaf, but also the ChlF emission. Increased chlorophyll levels in leaves lead to a rise in absorbed PAR (APAR), which in turn increases the ChlF emission from the leaf. Chlorophyll levels in leaves not only vary seasonally, but also diurnally (García-Plazaola et al 2017), between species (Li et al. 2018), as well as between sun and shade leaves (Niinemets et al. 2002). Although higher leaf chlorophyll levels increase the ChlF emission, the relation is complicated by (i) the chlorophyll distribution within the leaf, (ii) the escape probability (f_{esc}) of the photon emitted by the chlorophyll molecule and (iii) chlorophyll re-absorption present when Cab levels are high. The f_{esc} value estimates the escape probability of the ChlF emission escaping the leaf

and reaching the sensor, affected both by leaf chlorophyll concentration and leaf architectural properties (Buschmann, 2007). In chlorophyll re-absorption, the red ChlF emission is partially re-absorbed by the leaf chlorophyll when leaf chlorophyll contents increase. This is due to the absorption maxima of a leaf being near 680 nm, close to the red ChlF emission peak. This absorption quickly decreases with increasing wavelength and as such affects the far-red ChlF emission to a much lesser degree (Buschmann, 2007). The level at which this re-absorption overtakes the overall increase in ChlF signal due to higher leaf chlorophyll content is dependent on the concentration of chlorophyll molecules within the leaf (Liu et al. 2019).

1.3.1 Spectral- and PAM-fluorescence

At the leaf level, ChlF can be measured using active or passive techniques, depending on the light source; active techniques use a known source of illumination (i.e. a halogen or LED light), while passive techniques use radiation from the sun. Leaf-level active techniques include spectral fluorescence and PAM –fluorescence, while solar induced fluorescence (SIF) is measured passively. At the canopy scale, fluorescence is often measured using SIF, but other techniques, such as LED-induced fluorescence (LEDIF) exist (Atherton et al. 2019a). Additionally, laser induced fluorescence (LIFT) techniques can be used at variable scales from the leaf up to 50 meters (Ananyev et al. 2005; Pieruschka et al. 2010), but are not the focus of this study. While PAM-fluorescence measurements integrate the ChlF signal of around 60 nm, from 720-780 nm (Schreiber, 2004), spectral fluorescence allows for the measurement of the whole fluorescence emission spectra (Rajewicz et al. 2023). Furthermore, in contrast to spectral and PAM-ChlF measurements, SIF is retrieved using narrow, atmospheric absorption of Fraunhofer (solar) bands (Meroni et al. 2009, Aasen et al. 2019).

The full fluorescence spectra recorded by spectral fluorescence measurements allows the investigation of the shape of the fluorescence emission, specifically the shape of the two fluorescence emission peaks. The shape of the fluorescence spectra is modulated through PQ and NPQ dynamics (Rajewicz et al. 2023), PSI contribution to the ChlF emission (Pfündel 1998, Franck et al. 2002) and changes in the partitioning of energy between PSI and PSII (Porcar-Castell et al. 2014; Franck et al. 2002). The relationship between red and far-red ChlF emission can vary on the diurnal (Agati et al. 1995) and seasonal scales (Zhang et al. 2019; Rajewicz et al. 2023). The diurnal changes in the red to far-red peak ratio are affected most by NPQ and photosynthetic downregulation, while at the seasonal scale the changes are driven by leaf area and chlorophyll concentration (Zhang et al. 2019; Rajewicz et al. 2023). Finally, the fluorescence emission shape is also affected by the chlorophyll content of the leaf affecting both the absorption characteristic of the leaf as well as ChlF reabsorption (Agati et al. 1993; Cordon & Lagorio, 2006; Buschmann, 2007). Re-absorption alters the ChlF emission shape by decreasing the red peak emission, while having a minimal effect on the far-red emission peak, thus decreasing the red to far-red peak ratio.

Using the PAM-ChlF measurement method, it is possible to estimate the quenching parameters of the leaf, allowing us to connect PAM-ChlF measurements directly to the photochemistry of the leaf. The PAM-measurements are conducted by measuring both the minimum level (F_0) as well as the maximum level (F_M) of ChlF from the leaf. This is done by dark adapting the leaf, which causes the quinone acceptors in the leaf to be maximally oxidized, and the PSII reaction centers are considered to be open (Schreiber 2004). In this state, F_0 is recorded with a weak, non-actinic measuring light. The leaf is then given an

intensive pulse of light, which reduces the quinone acceptors, allowing for the recording of F_M , the maximum level of ChlF. Variations in the levels between F_0 and F_M can be used to convey information on the photochemistry of the plant, i.e. the lower the difference between these two values, the more stressed the plant is. This information is conveyed in the F_v/F_M parameter, the maximum quantum yield of photochemistry, which has been found to be lower in stressed plants (Kitajima & Butler, 1975; Demmig-Adams & Adams, 2006). The F_v/F_M parameter is calculated as the direct ratio between variable fluorescence ($F_v = F_M - F_0$) and F_M (Kitajima & Butler, 1975). Additionally, based on the F_0 and F_M values measured with PAM fluorescence, Genty et al. (1989) presented the quantum yield of photochemistry, the $Y(II)$ parameter ($Y(II) = 1 - (F / F_M)$, where F is steady state fluorescence), which was developed as an indicator of the amount of energy used for photochemistry in PSII. Related to the $Y(II)$ is the linear electron transport rate (ETR), which can be linked to the production of ATP and NADPH in the Calvin cycle, and is calculated as:

$$ETR = PAR \times Y(II) \times Abs \times \alpha_{II} \text{ Eq. 1}$$

Where α_{II} stands for the partitioning of energy into PSII, PAR for photosynthetically active radiation at the leaf surface and Abs for the absorption by the leaf. Together, PAR and Abs form APAR, although generally in ETR calculations the true APAR is not known and an absorption coefficient of 0.84-0.85 is used instead (Baker, 2008). However, PAR absorption does not stay constant in variable pigment compositions (Blache et al. 2011), possibly affecting ETR calculations. Additionally, while α_{II} is assumed to have a constant value of 0.5, α_{II} has been shown to vary due to the relative amounts of PSI and PSII (Laisk & Loreto, 1996) as well as different absorbance spectra of PSI and PSII (McClain & Sharkey, 2020). These assumptions provide a source of error for the ETR calculation in variable environmental conditions (Maxwell & Johnson, 2000).

Through ETR and its connection to ATP and NADPH production, PAM-fluorescence measurements form a link between the light and carbon reactions of photosynthesis (Krall & Edwards, 1992, Klughammer & Schreiber, 1994). As such, the concurrent measurements of ChlF and gas exchange have been used to formulate a more complete view on the relationships between carbon and light reactions of photosynthesis (Cornic & Briantais, 1991; Laisk & Loreto, 1996). Further research has been done on the partitioning of electrons to RuBisCO carboxylation/oxygenation reactions and alternative energy sinks (Laisk & Loreto, 1996; Morfopoulos et al. 2014), dynamics of mesophyll conductance (Flexas et al. 2007) and respiration (Yin et al. 2009). Measurements of both ChlF and gas exchange parameters, allow for the calculation of the ETR/A_{NET} (where A_{NET} stands for net carbon assimilation) proxy, which is used to estimate the rate of energy conversion between light and carbon reactions of photosynthesis (Krall & Edwards 1992; Flexas et al., 2002; Perera-Castro & Flexas 2023).

While PAM-fluorescence techniques have seen widespread application in investigating the energy partitioning and estimating the quantum yield of photochemistry in leaves, due to the measurement process requiring high-intensity light pulses, PAM-measurements are limited to the leaf scale. However, SIF methods are opening new opportunities in ChlF measurements, allowing for measurements across variable scales from the leaf to the canopy and beyond. While the connection of photosynthesis with PAM-fluorescence has been well documented, its connection with SIF is not straightforward. Relating the PAM and SIF measurements would require the quantification of the processes that connect the measured ChlF emission to photosynthesis, such as energy partitioning in PSII, distribution of energy

between PSI and PSII and the dynamics of alternative energy sinks. Additionally, spectral fluorescence measurements, with the information it carries on the changes of red and far-red fluorescence, could be used to connect PAM and SIF measurements.

1.3.2 Solar induced fluorescence

ChlF can be measured passively on the leaf and canopy scales using SIF. SIF is often measured using hyperspectral systems or systems specifically built for SIF measurements (Meroni et al. 2009; MacArthur et al. 2014). What makes SIF such a valuable tool in vegetation remote sensing is its potential to monitor both evergreen vegetation and gross primary productivity (GPP) (Porcar-Castell, 2014; Sun et al, 2017; Gu et al. 2019) at large scales. However, reflected light from the vegetation makes disentangling the reflectance and ChlF signals difficult, complicating SIF measurements. For this reason, SIF retrieval was first conducted using the Fraunhofer line depth (FLD) method, while more recent research has used the more complex spectral fitting method (SFM) (Meroni et al. 2009). The FLD methods, used in satellite remote sensing, made use of the different relative contribution of ChlF to the irradiance inside and outside of the absorption features (Theisen, 2002), while in SFM, mathematical models are used to disentangle ChlF and reflectance from radiance emerging from the vegetation (Meroni & Colombo, 2006) over a selected spectral range.

The retrieval of SIF is very relevant in the current photosynthesis research to be able to utilize SIF as a proxy of photosynthesis (Frankenberg et al. 2011; Sun et al. 2018) and plant stress (Helm et al. 2020; De Cannière et al. 2022). While taking into account both photosynthetic and canopy factors (Guanter et al. 2014), SIF can be presented as:

$$SIF = APAR \times \phi_F \times f_{esc} \text{ Eq. 2}$$

where APAR is the absorbed photosynthetically active radiation, ϕ_F the canopy level fluorescence quantum efficiency and f_{esc} , the escape probability of the ChlF emission in the direction of the sensor (Huang et al. 2007; Guanter et al. 2014). It is worth mentioning that f_{esc} can be approached both from the leaf level and canopy level perspectives, affected by different factors. The relationship between remotely sensed measurements of photosynthesis and SIF is mediated by changes in absorbed solar radiation (APAR) and photosynthetic light use efficiency (LUE) (Peng et al. 2011). These relationships are quantified in Monteith's (1972) LUE model ($LUE = GPP/APAR$), which we can combine with the SIF model (Eq. 2) to establish the equation describing the relationship between gross primary production and SIF (Martini et al. 2019; Dechant et al. 2020; Zhang et al. 2020):

$$GPP = \frac{LUE}{\phi_F} \times \frac{1}{f_{esc}} \times SIF \text{ Eq. 3}$$

Importantly, the relationship between GPP and SIF depends both on structural factors, such as the escape probability of the ChlF emission, and mechanistic factors, such as fluorescence efficiency (Eq. 3). While the LUE parameter integrates the responses across the whole photosynthetic process, changes in ϕ_F are modulated through radiation energy partitioning within the leaf, as it is affected by changes PQ and NPQ. In low light conditions, when a plant is in a "normal" state, i.e. not suffering from sustained stress, ϕ_F is controlled by PQ and is inversely related to the quantum yield from PSII (Van der Tol et al. 2014; Porcar-Castell et al. 2014). In a combination of high light conditions and low temperatures, such as on a cold and sunny winter day, NPQ decreases both the quantum yield, as well as

ϕ_F . In this case, since photosynthesis is affected by winter downregulation, the decreased utilization of absorbed radiation energy leads to an increase in NPQ (Demmig-Adams and Adams, 2006). The relationship between LUE and ϕ_F is also affected by alternative energy sink dynamics, which compete for electron transport with GPP, thus reducing LUE, but affecting ϕ_F to a much lesser degree (Porcar-Castell et al. 2014). Whether measuring spectral, PAM-ChlF or SIF, the origin of the ChlF signal is always the same. The light is first absorbed by chlorophyll molecules, after which it can either be used to power photosynthesis, dissipated as heat or re-emitted as chlorophyll fluorescence. Since these processes are complementary to each other, changes in one of these pathways affect the other pathways as well (Butler, 1978; Maxwell & Johnson, 2000). For this reason, it is important to understand the processes that affect both PQ and NPQ and the partitioning of light inside leaves. As excess light energy absorbed by the photosystems can damage the photosynthetic machinery (Tyystjärvi, 2013), plants continuously regulate the energy balance between light and carbon reactions via regulatory mechanisms (Demmig-Adams & Adams, 2006). This regulation of energy results in the performance of light reactions of photosynthesis following closely that of the carbon reactions, which forms the basis of remote sensing of photosynthesis through ChlF measurements (Porcar-Castell et al. 2014). Through this connection to plant photosynthesis, the measuring of SIF is of great value, as it allows for large-scale measurements of photosynthesis. However, when measuring SIF at the canopy and ecosystem scale, the ChlF emission of individual leaves is not resolved and as such, numerous factors, as well as their variability on temporal and spatial scales, must be taken into account, looked at more closely in the following chapters.

1.4 Interpretation of the physiological mechanisms affecting leaf spectral emission

The emission of spectral signals originating from leaves are modulated by the physiological properties and mechanisms of the leaf, such as pigment composition (Gitelson et al. 2005), APAR, and ChlF quenching dynamics (Porcar-Castell et al. 2014). Thus, co-registering of the short- and long-term changes of these mechanisms, in tandem with optical measurements, is key to understanding the mechanistic processes underlying the spectral signals. In reflectance based vegetation indices, such as NDVI, PRI and CCI, the signal is driven both by chlorophyll and carotenoid pigments as well as leaf and canopy structure. As such, the pigment composition and distribution of the leaves dictate the absorption and reflectance characteristics and spectra of the leaf (Maas & Dunlap, 1989; Datt, 1998), which, together with canopy structural effects, form the spectral signal reaching the sensor. This makes it important to understand both the seasonal variation of pigments, as well as the role of nutrient uptake in pigment formation. While CCI was originally formulated to track evergreen photosynthesis dynamics, both PRI and CCI have been found to correlate with changes in the xanthophyll pigments (Gamon et al. 1992; Gamon et al. 2016). The link between these two indices and the xanthophyll cycle, which in turn has been associated with leaf heat dissipation (Panigada et al. 2014), forms a link with NPQ dynamics (Evain et al. 2004, Porcar-Castell et al. 2012). While the seasonal dynamics of this relationship still has open questions, PRI and CCI, through their coupling to leaf dissipation and APAR dynamics, can help resolve some of the uncertainties related to changes in vegetation on a temporal scale. In addition to chlorophyll pigments, the ChlF emission is affected by the photochemistry of the plant

(Baker, 2008; Porcar-Castell et al. 2014). This makes the quantification of photosynthesis regulation a point of interest in remote sensing research.

Photosynthesis at the leaf level can be measured using, for example, shoot gas exchange chambers (Hari et al. 1999, Kolari et al. 2014) and open gas analyzer systems (Cornic & Briantais, 1991) in combination with PAM-fluorescence measurements. Portable infrared gas analyzer (IRGA) -systems exist for combined gas exchange and ChlF measurements, however, they are not suitable for long term field observations. While gas exchange chambers cannot directly be scaled up to the ecosystem level, eddy covariance techniques provide a powerful technique to study ecosystem-atmosphere interactions and GPP (Aubinet et al. 2012). However, eddy covariance measurements can be complex to setup, while being prone to data gaps and requiring ecosystem-specific assumptions (Hollinger & Richardson, 2005). A need for novel methods for resolving the seasonal dynamics of photosynthesis regulation, using simultaneous measurements of carbon and light reactions of photosynthesis would thus be required.

PAM-fluorescence measurements have been proven to be a valuable tool in plant physiology and photosynthesis studies (Schreiber 2004), however the relationship between SIF and photosynthesis is not so straightforward and is affected by various factors. These factors include APAR_g, PSII energy partitioning, distribution of energy between PSI and PSII, alternative energy sinks and canopy structural factors, as well as the temporal dynamics of all these factors. While SIF has the potential to be used in large scale monitoring of plant photosynthesis, the SIF measurement itself does not contain enough information to calculate the quantum yield of photochemistry. The link between PAM and SIF measurements of ChlF is complicated by the different methodology used, as well as the different spatial and temporal domains where the information is gathered from (Porcar-Castell et al. 2014). Combined, integrated measurements of ChlF and gas exchange could thus help in gathering information about the long-term regulation of photosynthesis and could help bridge the gap between PAM and SIF measurements. Consequently, the important link connecting SIF measurements to photosynthesis is disentangling the information that the SIF signal contains about APAR and photosynthetic light use efficiency (LUE) (Porcar-Castell et al. 2014). Consequently, SIF could be used to estimate APAR since it does not suffer from the same limitations as reflectance based vegetation indices (Frankenberg et al. 2011, Yang et al. 2021). While SIF has been found to contain information on both APAR and LUE (Yang et al. 2015; Gu et al. 2019), disentangling these effects has proven to be problematic and quantification of the link between SIF, APAR and LUE is needed. Both the fluorescence emission (measured by SIF) and photochemical yield are affected by PQ and NPQ and have been shown to react similarly to water stress, for example (Flexas et al. 2000).

To conclude, spectral remote sensing signals are driven by leaf level mechanisms that change with environmental conditions. To be able to disentangle the effects of these underlying mechanisms on the remote sensing signal, it is important to understand and quantify them. As such, to aid understanding these physiological processes, simultaneous measurements of spectral data and plant functions, such as photosynthesis, are required. The leaf level physiological processes are propagated at higher scales, and without comprehensive understanding of the underlying processes, it will be challenging to draw relevant, quantitative conclusions from the remote sensing data.

1.4.1 ChlF imaging systems aid in the mechanistic understanding of the leaf physiology and ChlF relationship

As mentioned, the capability to measure photosynthesis at the leaf and ecosystem-levels already exists when using IRGA's and the eddy covariance techniques. These methods, however, lack the ability to resolve the spatial variability of photosynthetic dynamics at the leaf and canopy levels. Resolving this variability would help in the mechanistic understanding of the relationship between leaf physiological processes, such as photosynthesis and growth, and spectral remote sensing signals. Imaging systems based on ChlF sensors have the potential to fill this gap (Thomas et al. 2018). ChlF imaging is a rather recent advancement, where instead of a single spectrum, the sensor gathers images (Kaiser et al. 2013). ChlF imaging instruments, such as the Imaging-PAM (Heinz Walz GmbH, Effeltrich, Germany), provide a robust tool for resolving heterogeneity of the plant photosynthetic performance on a spatial scale in variable conditions, providing information on various scales (Rofle & Scholes, 2010). Fluorescence imaging has seen wide use in plant physiology, such as in pathogen detection (Rolfe and Scholes, 2010), mapping the dynamics between photosynthesis and growth (Walter et al. 2004), investigating spatiotemporal variation of photosynthesis (Rascher et al. 2001) and monitoring leaf diseases (Chaerle et al. 2007). When used in combination with IRGA-systems, the measurement of fluorescence imaging and gas exchange parameters allow for the direct comparison between ETR and the rate of CO₂ assimilation as key indicators of in situ photosynthetic performance of plants (Berger et al. 2007). This allows for the mapping of the relative contributions of the different parts of the leaf to the CO₂ assimilation (Chou et al. 2000; Swarbrick et al. 2006). An additional caveat for the ChlF imaging system comes from the restrictive pricing of these systems.

Consequently, while not addressed in the three studies forming this thesis, the author has additionally contributed to the development of a novel, low cost fluorescence imaging device. The device, named "Low cost chlorophyll fluorescence imaging solution for precision plant stress and yield application" has been registered with the University of Helsinki with the invention disclosure number 1158/2021. The device integrates a miniature camera to a pocket computer, and by recording images, allows for the measurement of spatial variation of reflectance and ChlF emission. The capabilities of the sensor have been established in two different tests, where the emission measured by the sensor was compared to simultaneously gathered results from an Imaging-PAM system, as well as a PAM imaging setup at the Viikki Plant Phenotyping (NaPPI) facility. The development of this prototype sensor will continue in the future with potential applications in stress detection in vertical farming and plant phenotyping in tree nurseries. Originally, the object of the development was to add published articles about the invention to this thesis, but due to a conflict between potential future patenting and scientific publications, the development of the sensor was left out of the thesis publications.

1.5 Spatial variation affecting remote sensing signal interpretation

The leaf level mechanisms presented in the previous section set a foundation upon which to interpret the remote sensing signals (Malenovský et al. 2009). As such, when the remotely sensed signal containing plant functional information is propagated from the leaf to the

canopy scale, it is affected by spatial variability. The issue of scale in remote sensing has been a subject of discussion since the end of last century, coinciding with the proliferation of remote sensing measurements (Quattrochi & Goodchild, 1997; Marceau & Hay, 1999). One of the key strengths of spectral remote sensing of vegetation lies in its ability to examine how information changes with scale, and thus allows for the gathering of information about leaf physiological and ecosystem functions at variable temporal and spatial scales (Gamon et al. 2007). The intensity and spectral properties of the remote sensing signal are affected by changes in different factors, such as measurement geometry, atmospheric effects, reabsorption and canopy structure, making the remote sensing measurements dependent on the observer location and viewing geometry (Van der Tol et al. 2009). As these factors can work as either couplers or decouplers between the measured variable and the remote sensing signal, it is important to contextualize and quantify the effects that the variables have. Thus, to help us interpret the spatial scaling of the remote sensing signal requires understanding of the canopy-atmosphere radiative transfer properties of the spectral signal.

Remote measurements of ChlF and reflectance are affected by the canopy structure of the measured area. This includes leaf area, often measured by the leaf area index (LAI), as well as leaf inclination, often measured by leaf angle distribution (LAD), average leaf angle (ALA) or mean tilt angle (MTA). New technologies allow for the quantification of these parameters by combining satellite data and machine learning algorithms (Zou et al. 2022). Additionally, multi-scale data has been combined to measure fractional cover of green vegetation from UAV's and satellites (Riihimäki et al. 2019). Variation in these structural parameters is affected by environmental conditions, such as drought (Lahlou et al. 2003; Valladares & Pearcy, 1997) and nutrient availability (Yin et al. 2003), underlining the importance of quantifying the effects that these factors have on the canopy structure.

In addition to canopy structural factors and leaf amount and arrangement, spectral remote sensing measurements at the canopy level are affected by the amount and distribution of chlorophyll within a leaf. These factors are also the drivers of APARg, which connects SIF to photosynthesis at both leaf and canopy scales. When ChlF is emitted from the leaf, some of it is reabsorbed, either within the leaf, or within the canopy. The amount of ChlF emission reaching the remote sensing sensor (f_{esc}) thus depends on the leaf physiological variables (chlorophyll amount, morphology), as well as canopy structural variables. These factors act as decouplers between the SIF – photosynthesis relationship. In addition, independent of the object measured, the measurements are affected by viewing and illumination geometry, as well as the ratio of direct and diffuse radiation (Wu & Li, 2009). The radiation and illumination geometry effects are captured in the bidirectional reflectance distribution function (BRDF), which can help quantify the scattering of light in different canopy structures (Lucht & Roujean, 2000; Montes & Ureña, 2012). These directional scattering properties should be taken into account when comparing data from different observation geometries. The problems caused by scattering (Chen et al. 2003) as well as the sun-sensor geometry (Zeng et al. 2023) can be alleviated using multi-angle reflectance data, which can also be used to gather canopy structural information.

In an attempt to resolve the effects of plant structure on its ability to capture light and perform photosynthesis, functional-structural plant models (FSPMs) have been formulated (Sievänen et al. 2014). FSPM's are however unable to resolve canopy level fluxes due to heterogeneity in radiation interception in complex canopies (Bailey & Kent, 2021). Radiative transfer models (RTM), which are mathematical and computational tools to simulate and study the interactions of light with vegetation as it propagates through a canopy, have been developed to study these complications. They are used to interpret measurements of reflected

and emitted radiation from vegetation. RTM's take into account how radiation is influenced by interactions with vegetation, including absorption, multiple scattering, and emission, while considering wavelength of the radiation, as well as the geometry of the canopy (Gastellu-Etchegorry et al. 2004; Van der Tol et al. 2009). In vegetation remote sensing, radiative transfer models exist for the leaf (e.g. PROSPECT, Feret et al. 2008), canopy (e.g. Flight, North, 1996) and combined scales (e.g. SCOPE, van der Tol et al. 2009). While advancing our knowledge of the scattering of light in various physical environments, they require accurate input data to produce reliable results, not yet readily available due to limited multiscale field campaigns.

With the use of multisource data, such as combined RTM-modelling and multi-scale spectral measurements, it would be possible to quantify the effects that scaling the remote sensing signal from leaf to canopy has. Novel methods, based on versatile and affordable UAV platforms, allow for simultaneous multiscale measurements, potentially helping connect leaf and satellite level measurements. With these advances, it would be possible to contextualize the effects of scaling, helping bridge the gap between plant physiological functions – such as photosynthesis – and remote sensing measurements, offering advances for not only remote sensing, but also photosynthesis modelling.

2. AIM OF THE STUDY

Through the use of novel methodology, this thesis aims to facilitate the interpretation of multiscale optical remote sensing measurements of spectral reflectance and SIF, connecting them to photosynthesis across variable spatial and temporal domains. This aim is reached with the following two distinct goals:

Goal 1: Quantify the physiological processes, as well as the regulatory mechanisms affecting them, that connect spectral measurements to photosynthesis and nutrient contents at the leaf level. (Studies II & III)

Goal 2: With the use of novel methods, investigate the impacts that spatial factors have on the spectral remote sensing of photosynthesis and leaf nutrients when scaling the signal from leaf to canopy (Studies I & II).

These goals are considered in the context of the three Studies included in this thesis. Consequently, we hypothesize that in water stressed conditions, the spatial and diurnal variation in SIF is controlled by both leaf (Φ_{F_PSII}) and canopy (LAD) level processes (Study I). Additionally, we postulate that photoprotection-related indices (PRI, CCI), along with ChlF will be more strongly correlated with foliar nutrients due to their close connections with leaf level physiological processes, when compared to vegetation indices based on vegetation greenness in Study II. Finally, in Study III, we introduce a novel instrument capable of tracking long term photosynthesis regulation *in situ* in variable environmental conditions, allowing for advances in photosynthesis modelling and remote sensing.

3. MATERIALS AND METHODS

3.1 Study sites and plant materials

The measurements described in this thesis were performed on two distinct sites. Firstly, for Studies I & II, an agricultural site on the Viikki Campus area in Helsinki, Southern Finland (60°23'N, 25°02' E) was selected for the cultivation of potato plants (*Solanum tuberosum* L., variety 'Lady Felicia') in the summer of 2018. The experiment included 16 nutrient fertilization plots with four different fertilization regimes: N1A1, N2A0, N2A1, N2A2(control) (Figure 2). The letter describes the fertilizer used (N= nitrogen fertilizer, A= fertilizer with micro- and macronutrients) and the number the amount of fertilizer used (0 = none, 1 = half the typical amount, 2 = typical fertilization level). In addition to the nutrient treatments, ten plots with control level nutrients were used as a water stress experiment, organized as a split plot design using five replicates of both irrigated and non-irrigated plots (I+ & I-, Figure 2). Planted at the end of May in 6 x 6 m plots, all the plots were irrigated until 2.7., when the water stress experiment started, after which only half the water stress experiment (I+) and all the nutrient experiment plots were irrigated with a combination of sprinkler and furrow irrigation. Data collection for Studies I & II were conducted on the 10.-11.7.2018, 17.-18.7.2018 and 25.-25.7.2018. For the leaf level measurements in Studies I and II, fully developed, top canopy leaves were randomly sampled for both field and laboratory measurements. Top canopy leaves were chosen for an optimal match with the canopy level measurements conducted from the UAV and hydraulic lift (See section 3.3).

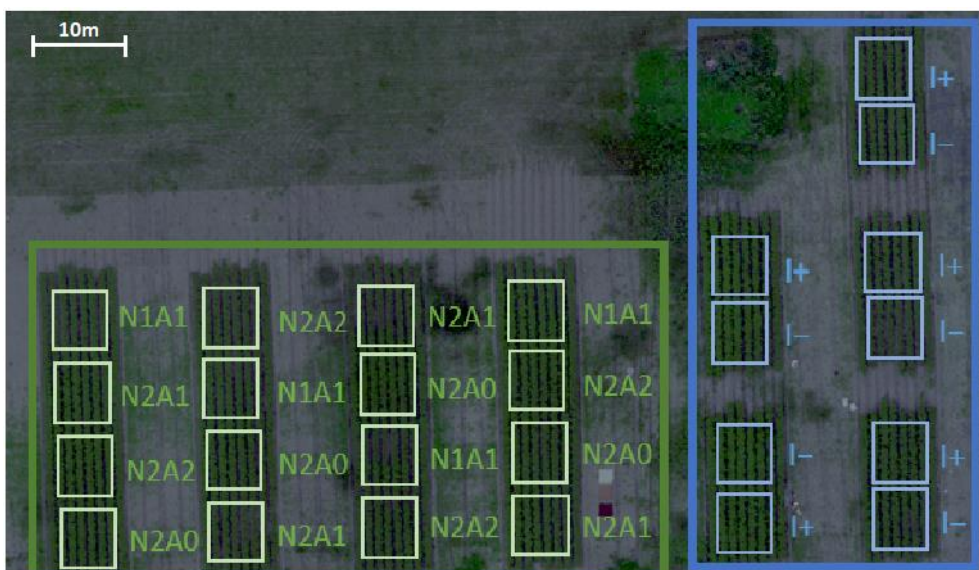


Figure 2 Overview of the plot distribution used in Studies I & II. I+ & I- refer to the water stress experiment plots located inside the blue area, while the plots inside the green area refer to the nutrient fertilizer experiment plots and the variation of the fertilizer treatment, detailed in section 3.1. Figure adapted from Study II.

Furthermore, in Study III, wherein we introduce a first demonstration of integrated PAM-ChlF and gas exchange field measurements, we chose a 60-year-old silver birch (*Betula pendula*, Roth) tree located at the SMEAR-II station (Station for Measuring Forest-Ecosystem-Atmosphere Relations) in Southern Finland (61°51' N, 24°17' E). The measurements were conducted between 29.6. – 9.8.2021 on two top canopy shoots, facing towards south or south-west for optimal lighting conditions. These shoots were used for the combined measurements of ChlF and gas exchange parameters, as well as additional benchmarking measurements.

3.2 Leaf level measurements

3.2.1 Leaf optical measurements

Measurements of reflectance (Study II) and spectral fluorescence (Study II) were performed in laboratory conditions, while PAM fluorescence measurements (Study I & Study III) were performed in field conditions.

To estimate a range of vegetation indices, we measured the leaf directional-hemispherical reflectance spectra in laboratory conditions using a RTS-3ZC Integrating Sphere (ASD Inc., Boulder, CO, USA) connected to an ASD Hand-Held Spectrometer (ASD Inc., Boulder, CO, USA). The spectrometer has a range (R) of 325-1075 nm, sampling interval (SI) of 1.6 nm and a full width at half maximum (FWHM) of 3.5 nm. A dark current was subtracted from the measurements, and leaf direction-hemispherical factors were calculated with the aid of a Spectralon® panel (Labsphere, North Sutton, NH, USA). To measure spectral fluorescence, we used a USB-2000+ spectrometer (Ocean Optics Inc., Orlando, FL, USA) (R: 300-1100 nm, SI: 0.5 nm, FWHM: 1.5-1.8 nm) together with a halogen light source (HL-2000, Ocean Optics Inc.). Connected to the spectrometer was a bifurcated reflectance probe (R600-7-VIS-125F, Ocean Optics Inc.), which we used to conduct the spectral measurements from a nadir position. Furthermore, the probe was connected to a filter carrier, which held an optical



Figure 3 The Micro-PAM fluorometer fitted inside a shoot chamber system. This novel system allowed for the concurrent measurements of PAM-ChlF and gas exchange parameters.

density 4 short-pass 650 nm filter (Edmund Optics, Barrington, NJ, USA), blocking over 99% of radiation above the 650 nm wavelength.

For Study I, in order to measure steady state (F) and maximum fluorescence (F_M), PAM measurements were conducted in field conditions with the PAM-2500 (Heinz Walz GmbH, Effeltrich, Germany) fluorometer. These measurements used saturating pulses of 800 ms and ca. 8000 μmol and were synchronized with concurrent canopy level UAV and hydraulic lift measurements (section 3.3). Furthermore, for Study III, PAM-fluorescence was simultaneously measured using the MICRO-PAM (Heinz Walz GmbH) and MONI-PAM (Heinz Walz GmbH) systems in field conditions. Both of the above-mentioned measurements for Study III were conducted on different top canopy shoots, situated no more than 1 m from each other. To provide a more comprehensive view of photosynthesis regulation, we aimed for simultaneous co-registering of gas exchange and ChlF parameters, and so the ChlF measurements with the MICRO-PAM were performed just as the shoot chamber lid started to close. The MICRO-PAM device, used here for the first time fitted inside a dynamic shoot chamber system (Figure 3), used a blue measuring light. This measuring light, in addition to the saturating pulses (800 ms and ca. 6700 μmol) and the ChlF emission, were transmitted through a 10 cm long light guide, the tip of which was placed ca. 3-5 mm from the leaf surface, at a 35° angle from the leaf plane. Co-registering PAM-ChlF with the MICRO-PAM was a MONI-PAM device, which, unlike the MICRO-PAM, does not use a light guide. Instead, the measuring light is positioned 25 mm away from the measured leaf, which is attached to the device with a clip. In addition, the MONI-PAM is larger, preventing it to be fitted inside a shoot chamber. Both of these devices were operated through a MONI-DA data acquisition system (Heinz Walz GmbH) and measured F and F_M , used to calculate the quantum yield of effective photochemistry of PSII (Y(II)) and, subsequently, electron transport rate (ETR) (see section 1.3).

3.2.2 Foliar pigment, nutrient and leaf area analysis

To study the temporal and spatial variation in foliar chlorophyll and carotenoid contents, pigment contents of fully developed, top canopy leaves were estimated for Studies I & II. Three plants were sampled from each plot (N = 3 replicates) on the 10.7., 16.7. and 25.7. The samples were placed in cryotubes and frozen in liquid nitrogen directly after sampling to prevent pigment deterioration. Before pigment determination, the samples were thawed, and 1.8 mL of dimethyl sulfoxide (DMSO) was added into the tubes. The samples were placed in a 50° C oven for eight hours to extract, and after cooling down, were centrifuged for 10 minutes at 3600 rpm (5810-R, Eppendorf, Hamburg, Germany). The resulting extract was analyzed with a spectrophotometer (Shimadzu UV-1800, Shimadzu Corporation, Kyoto, Japan). Chlorophyll and carotenoid pigment values were estimated from the absorbance of the extract at specific wavelengths, measured by the spectrophotometer, using equations from Wellburn (1994).

To determine the effects the different treatments had on the foliar nutrient contents, and how these different foliar nutrient levels were reflected in plant optical signals in Study II, we estimated the foliar nutrient contents of top canopy leaves. Plant material was gathered and stored similarly to the pigment estimation (see above) on 10. & 25.7.2018. Samples were then subsequently thawed and dried in an oven at 50° C. After homogenization, 200-300 mg (dry weight) of each sample was mixed with 10 mL of HNO_3 and 1 mL of H_2O_2 . The samples were digested in a MARS 5 – microwave digestion system (CEM Corporation, Matthews,

NC, USA) for 10 minutes at 175° C and consequently analyzed with an ICP-MS mass spectrometer (Thermo Fisher Scientific, Waltham, MA, USA), following the method by Thomas (2008). The nitrogen and carbon concentrations were studied separately, so that after drying and homogenization, 250 mg of each sample was analyzed using a Variomax CN Analyzer (Elementar Analysensysteme, Hanau, Germany), using the dry combustion method, detailed in Bremner et al. (1996).

Finally, to investigate changes in leaf morphology, we calculated the specific leaf area (SLA) for each plot, calculated as projected leaf area (cm²) divided by leaf dry weight (g). Fresh leaves (N = 9) from each plot were scanned on top of a white paper including a ruler for scale, which allowed for the calculation of the leaf area using the GNU image manipulation software (GIMP development team, 2021). After scanning, the leaves were dried in a 50° C oven until dry and weighed.

3.2.3 Leaf gas exchange measurements

Photosynthetic gas exchange measurements were performed in Studies I & III. In Study III, the net assimilation rate was calculated directly by the gas exchange system. In Study I, leaf stomatal conductance (g_s) was measured with a leaf porometer (AP4 Porometer, Delta-T Devices, Cambridge, U.K.) from 10 randomly sampled top canopy leaves. Additionally, light responses and A-C_i curves were measured from three replicates from the control and water stress plots using the GFS-3000 (Heinz Walz GmbH). Using results from these measurements, A_{NET} (μmol m⁻² s⁻¹) was estimated based on the Ball-Berry model (Ball et al. 1987) as follows:

$$A_{NET} = \frac{G_s \times C_s}{m \times RH} \text{ Eq. 4}$$

Where G_s (mmol m⁻² s⁻¹) stands for the measured stomatal conductance, C_s for the air CO₂ concentration (assumed here to be 415 ppm), RH (%) for relative humidity, and finally m for the slope of the relationship between G_s and $A \times RH/C_s$ (the Ball-index) (Ball et al. 1987). With the addition of daytime respiration (R_d), assumed to be the rate of CO₂ measured at zero PAR at similar temperatures, GPP was calculated. It is worth noting that this assumption in daytime respiration may lead to a small overestimation of GPP due to the Kok effect (Sharp et al. 1984).

$$GPP = A_{NET} + R_d \text{ Eq. 5}$$

In Study III, gas exchange measurements were performed with a dynamic shoot chamber cuvette connected to a nearby IRGA system (LI-840A, Li-Cor Inc., Inc., Lincoln, Nevada, USA). The measurements were conducted with a top canopy silver birch shoot. Inside the chamber the birch shoot, arranged on a 2D plane, was kept in place by transparent fishing lines. The shoot chamber cuvette, which additionally housed a MICRO-PAM fluorometer (see section 3.2 & Figure 3), is a see-through acrylic box with a sliding lid. The chamber was kept open most of the time to expose the shoot to ambient conditions and closed only to measure gas concentrations for 60 seconds every 20 minutes. Through fluorinated ethylene propylene (FEP) tubing, the cuvette was connected to the central gas analyzer unit, which measured CO₂ and H₂O concentrations sent by the cuvette system. In addition to gas fluxes, the chamber system housed a quantum sensor for PAR readings, as well as a thermocouple for temperature readings. Additional technical details on the cuvette can be found in Kolari et al. (2014). Data used to calculate environmental variables was gathered from the nearby

SMEAR-II station: pressure readings from a barometer (Druck DPI 260, Baker Hughes, Houston, Texas, USA) and precipitation data from a weather sensor (Vaisala FD12P, Vaisala, Vantaa, Finland).

These added environmental measurements allowed us to calculate stomatal conductance (g_s), saturated vapor pressure (SVP) and vapor pressure deficit (VPD). The Magnus-Tetens equation (Tetens, 1930; Monteith & Unsworth, 1994) was first used to calculate SVP (kPa) relative to temperature:

$$SVP = 0.61078 \exp \frac{17.27 \times T}{T + 237.3} \text{ Eq. 6}$$

where T is the temperature inside the chamber (°C). Additionally, following the ideal gas law, vapor pressure (VP) (kPa) was calculated using the ambient H₂O concentration and temperature inside the chamber. Having calculated both SVP and VP allowed us to calculate VPD (kPa) as:

$$VPD = SVP - VP \text{ Eq. 7}$$

This in turn allowed us to estimate g_s , calculated as:

$$g_s = \frac{E}{VPD} \times P \text{ Eq. 8}$$

where g_s stands for stomatal conductance (mmol m⁻² s⁻¹), E for the transpiration rate (mmol m⁻² s⁻¹) measured by the gas exchange system and P for atmospheric pressure (kPa).

3.3 Canopy level measurements

3.3.1 Canopy level optical measurements

To study how spectral signals scaled from the leaf to the canopy scale, canopy level measurements of reflectance and SIF were performed (Studies I&II). The measurements were conducted using an UAV (Studies I & II), as well as a hydraulic lift system (Study I). The UAV measurements were conducted on five different occasions: 10.7 & 11.7.2018 (Study II), 17.7 & 18.7.2018 (Study I) and 25.7.2018 (Study II). Both the UAV and the hydraulic lift were in turn fitted with the Piccolo Doppio dual field-of-view system (Atherton et al. 2018; Porcar-Castell et al. 2015; MacArthur et al. 2014), as well as a GoPro camera, mounted in nadir position into a gimbal stabilization system (Photohigher, Wellington, New Zealand), allowing for the verification of correct measurement position. The UAV, which was based on a Gryphon Dynamics frame, flew ca. eight meters above the canopy, and collected data with a 25° field-of-view, cosine corrected bifurcated fiber, resulting in a 1.77 m radius footprint. The UAV hovered for approximately one minute above each plot. This resulted in 25 measurements per plot, which were then averaged for further data analysis, after correcting for the dark current.

The dual field-of-view Piccolo Doppio housed two spectrometers, the QE Pro (Ocean Insight Inc., Dunedin, FL, USA) (R: 640-800 nm, SI:0.16 nm, FWHM: 0.31 nm) and the Flame (Ocean Insight Inc.) (R: 340-1000 nm, SI: 0.33 nm, FWHM: 1.3 nm). Due to its wider range, the Flame spectrometer was used for estimating canopy reflectance in the visible and near-infrared range in Study II, while the QE Pro was used for estimating canopy SIF in both

Studies. The integration times of the measurements were automatically set by the system based on illumination conditions. Vegetation indices were estimated according to the calculations presented in Table 1.

Data on the diurnal dynamics of SIF in Study I was additionally gathered with the Piccolo Doppio attached to a hydraulic lift system. These measurements were collected at the same height as the canopy optical measurements, resulting in the same measuring footprint. These measurements were conducted on 18.7. and only on the water stress experiment plots, measuring each plot for 20 minutes.

3.3.2 SIF retrieval and processing

In both studies, SIF was retrieved using the Spectral Fitting Method (SFM) using the Earth's two O₂ absorption features, the O₂β (687 nm) and O₂α (760 nm) bands, situated in the spectral proximity of the two fluorescence emission peaks (Pérez-Priego et al. 2005; Meroni & Colombo, 2006). A small offset of 0.03 nm was found at the O₂α feature, which was corrected using an interpolation-based technique described in Atherton et al. (2019b). Additionally in Study II, to factor in the potential variation in irradiance caused by changing illumination conditions during various measurements, SIF yield was estimated as follows:

$$SIF_{YIELD} = \frac{SIF}{E_{PAR}} \text{ Eq. 9}$$

Where E_{PAR} is the irradiance (W / m²) integrated from the PAR region, between 400 and 700 nm.

3.3.3 Estimation of canopy structural parameters

To study how canopy structure affects the scaling of spectral signals when moving from the leaf to the canopy scale, structural parameters were estimated both from ground measurements and from the UAV from a height of 50 m. From the ground, the LAI in Study I was calculated using the pin-point method (Jonasson, 1988), in which lines are drawn diagonally through a plot and sampled at 50 cm intervals. At these 14 randomly distributed points, we calculated the number of leaves that were intercepted if a sharp weight was dropped from each point towards the ground. The canopy LAI was the average number of interceptions calculated from all these points. However, it is important to note that the pin-point method tends to underestimate the total projected LAI. Due to logistical difficulties, the pin-point method was unavailable to use in Study II.

In Study II, the remote estimation of structural parameters was conducted by gathering multispectral data with the MicaSense RedEdge M (AgEagle Sensor Systems Inc., Wichita, Kansas, USA) multispectral sensor. In Study I, two Sony A7R II digital cameras fitted with Sony FE 35 mm f/2.8 Carl Zeiss Sonnar T* lenses were used to gather point cloud data. The cameras were placed at 15° oblique angles from the vertical plane and the data gathered was used to build a detailed 3D reconstruction of the canopy. Consequently, different structural parameters were estimated. In Study I, canopy structure dynamics were estimated using Leaf area index (LAI) and leaf angle distribution (LAD), while in Study II, fractional vegetation cover (FVC) was used to track the development of the canopy structure.

Furthermore, LAD was estimated using two methods; a ground based photographic method (Pisek et al. 2011), as well as a new method (Xu et al. 2020) based on estimating

LAD from point clouds. In the first method, a diurnal dataset of LAD was gathered from plots W7 & W8 using a cell phone camera (Honor 9, Huawei Technology Co., Ltd., Shenzhen, PRC) secured to a tripod. The camera was placed perpendicular to the ground, ca. 50 cm outside the plot edge. Using one-hour intervals, we took pictures of three different sections of plants. From these pictures, the average leaf inclination angle (ALA) was determined with the aid of the ImageJ software (<http://rsb.info.nih.gov/ij/>), after Pisek et al. (2011). To model changes in LAD on the diurnal scale, a two-parameter leaf inclination distribution function (LIDF) was used after Verhoef (1998):

$$LIDFa = \frac{(45^\circ - ALA) \times \pi^2}{360} \text{ Eq. 10}$$

Subsequently, using Verhoef's leaf angle algorithm, LAD was estimated using LIDFa, as well as LIDFb, which was fitted with LAD estimated from point cloud data. In the new method, LAD data was gathered using the Structure from Motion (SfM) photogrammetric method, collected using the UAV fitted with digital cameras for spatial dimension information. In the SfM method, as described in more detail in Xu et al. (2020), LAD was retrieved directly from the point cloud data by classifying leaf and soil from each plot separately according to point height.

Finally, we estimated the canopy fluorescence escape probability (f_{esc}), which affects the relationship between SIF and GPP. The factor f_{esc} , which is dependent on LAD, was estimated using near infrared of vegetation (NIRv) and the fluorescence correction index (FCVI), according to Zeng et al. (2019). This estimation requires the knowledge of fAPAR, which in our case was estimated through a Rededge_NDVI proxy (Viña & Gitelson, 2005).

In Study II, to track the development of the crop canopy, FVC was estimated from multispectral images collected with the RedEdge M sensor on 10.7 and 25.7. The images collected by the sensor were processed to orthomosaics using the Agisoft PhotoScan Professional commercial software (AgiSoft LLC, St. Petersburg, Russia) with a ground sample distance of 3.55 cm. Using the histogram-based segmentation method with the QGIS-program (QGIS Geographic Information System, QGIS Association, <http://www.qgis.org> (accessed on 1 September 2022)), we classified each pixel in the plot areas to 0 s and 1 s according to their reflectance in NIR-band (center wavelength 842 nm, bandwidth 57 nm). This segmentation allowed us to subsequently estimate the FVC for each plot, calculated as the ratio of the canopy pixels (1 s) to the total pixel amount (0 s+1 s). Although aware of the problems the NIR band could have in full canopy conditions (Gitelson et al. 2002) due to uncertainties in the gathered visible wavelength data, we decided to use the NIR-band only.

3.3.4 Radiative transfer model

In order to separate the causes of SIF variation on the temporal and spatial scales in our canopy level measurements, a sensitivity-based analysis was performed in the combined radiative transfer model SCOPE (v 1.73). This analysis was focused on LAD and the quantum efficiency of PSII, since they were assumed to be the main drivers of the SIF signal. We generated several scenarios where LAD and quantum efficiency of PSII were either kept constant or were following the measured dynamics. The scenarios had three objectives: To quantify the importance of LAD and of quantum efficiency of PSII on the 1) diurnal and 2) spatial variation of canopy level SIF, and 3) their relative contribution to the relationship between SIF and GPP. Furthermore, a sensitivity index was calculated based on differences

in SIF under different scenarios, thus quantifying the influence of LAD and quantum efficiency of PSII on diurnal and spatial variation. Diurnal variation scenario predictions were validated against measurements from the lift platform, while spatial variation scenario predictions were validated against the SIF measurements from UAV observations.

4. RESULTS

This thesis investigates two inherent issues concerning the remote sensing of photosynthesis and nutrients. Firstly, In Section 4.1, we connect the leaf spectral signals to the leaf physiological processes by quantifying these processes and their changes on a temporal scale. In Study I these interactions are investigated by exploring the relationship between SIF and GPP with leaf and canopy level measurements. In study II, we investigate how differences in a variety of micro- and macronutrient levels, brought on by nutrient and water stress, affect the pigment composition of the leaf and consequently their spectral signature. Finally, in study III we measure both PAM-fluorescence and gas exchange parameters simultaneously, looking into the distribution of energy into carbon and light reactions within the leaf in the context of long-term regulation of photosynthesis. We explore how the responses of these reactions differ in changing environmental conditions and underline some of the important factors modulating leaf photochemistry and fluorescence quenching dynamics.

Secondly, in Section 4.2, we investigate the spatial factors affecting the spectral remote sensing measurements, when the signal is scaled from leaf to the canopy. In Study I, SIF was both measured and simulated to investigate the spatial and diurnal variation of SIF in response to water stress. Additionally, we investigated how water stress affected the relationship between SIF and GPP through changes in LAD and LAI. In Study II, both reflectance based vegetation indices and canopy level SIF were used to investigate how different leaf nutrient levels were detected in spectral measurements on both the leaf and canopy scales when affected by both fertilizer and water stress treatments.

4.1 New methods to connect physiological processes to spectral signals at the leaf level

Through Studies I, II and III, we aimed to investigate the physiological processes that connect leaf level spectral measurements to photosynthesis and leaf nutrient contents. In Study I the aim was to investigate how water stress affects the relationship between structural and photosynthetic factors and SIF, connecting spectral measurements and photosynthetic factors at the leaf level. We hypothesized that the diurnal and spatial variation of SIF would be controlled by quantum yield of fluorescence in PSII (Φ_{F_PSII}) and LAD. Thus, both leaf and canopy level data were gathered with the goal of quantifying the relative effects that canopy structural and leaf photosynthetic dynamics have on the temporal and spatial variation of SIF in potato crops. At the leaf level, as was expected, the measured photosynthetic parameters Φ_{F_PSII} , F_v/F_M and operating quantum yield of photochemistry in PSII (Φ_p) were higher in control plots relative to the treatment plots suffering from water stress. The SIF emission was found to be higher in the control plots, as stressed treatment plots had higher average leaf angle (ALA) and NPQ. Additionally, we estimated the influence of leaf angle distribution

(LAD) and the quantum yield of fluorescence in (Φ_{F_PSII}) on the SIF-GPP relationship. According to our simulation results, after considering changes in APAR caused by sun angle, both Φ_{F_PSII} and LAD were of similar importance (44-58 % and 42-56 %, respectively) when determining their effect on the diurnal response of SIF to water stress (Study I, Figure 7). The effects of water stress on canopy structure are further discussed in Section 4.2.

In Study II, we aimed to characterize the relationship between reflectance based vegetation indices, SIF and changes in foliar contents of a variety of micro- and macronutrients. The novelty of the research stemmed from using combined UAV and leaf level spectral measurements of 11 different micro- and macronutrients. A fertilization treatment using a variety of micro- and macronutrients was combined with a water stress experiment to investigate the spatial variation of nutrients in potato crops. We hypothesized that due to their more direct link to leaf physiology and PAR dynamics, the photoprotection-related indices PRI and CCI, as well as ChlF, would be more strongly correlated with leaf nutrients than more traditional, greenness-based indices, such as NDVI.

From the results of Study II, we found that the measured nutrients could be divided into two groups, based on whether they increased or decreased during the study period. Group 1 nutrients (potassium, magnesium, phosphorus and nitrogen) decreased in all treatments over

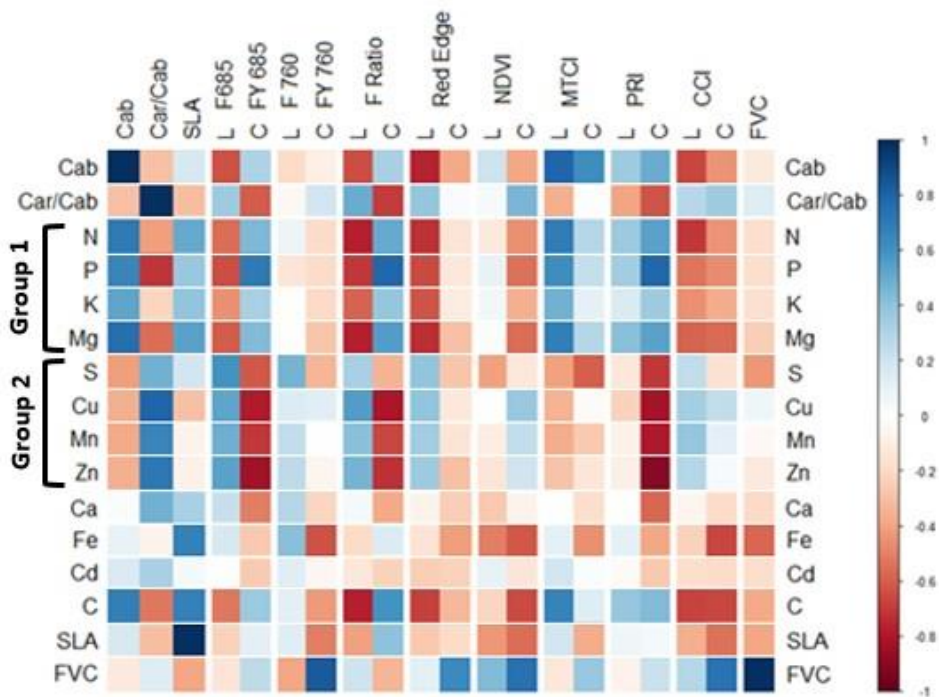


Figure 4 Correlation matrix comparing leaf (L) and canopy (C) level spectral indices to leaf level nutrient and pigment contents. If the color of the correlation between the leaf and canopy stays the same when moving from the leaf to the canopy, it indicates that the sign of the correlation scales up. If the color changes between the scales, the correlation is reversed when moving from one scale to another. The data used in the matrix is a combination of early and late measurement points ($n = 52$). Color denotes the Pearson correlation coefficient R-value, which is explained in the color chart on the right. All colored (non-white) squares are significant at the p 0.05 level. Figure adapted from Study II.

time as a response to canopy development, while Group 2 nutrients (sulfur, copper, manganese and zinc) increased. Leaf chlorophyll contents in top leaves remained stable between the treatments as well as during the measurement period, with chlorophyll content only decreasing in the water experiment control plots. Leaf chlorophyll and nitrogen contents were found to be positively correlated throughout the study, which is in line with the well-established role of nitrogen as an important building block of the chlorophyll molecule (Evans, 1989). At the leaf level, strong correlations could be noted between leaf red edge reflectance, MTCI and Group 1 nutrients, stemming from the connection red edge has to the leaf chlorophyll contents (Horler et al, 1983). Expectedly, the PRI was negatively correlated with the increased levels of protective carotenoid pigments compared to leaf chlorophyll (Car/Cab – ratio), while the CCI, however had a weak positive correlation with it. On the leaf level, the PRI was only weakly positively correlated with changes in Group 1 nutrients, while CCI had a strong negative correlation with nitrogen (Figure 4).

The red fluorescence peak emission (F685) and the fluorescence peak ratio (Fratio) were both negatively correlated with foliar chlorophyll contents and Group 1 nutrients. The far-red fluorescence peak emission was not correlated with any of the nutrients or pigments at the leaf level. While nitrogen has been known to be detectable in leaf level measurements of PAM, red, and the red to far-red peak ratio fluorescence (Wang et al. 2022; Jia et al. 2018; Agati et al. 2013), the relationship can change due to re-absorption and leaf physiological process dynamics (Ač et al. 2015). We extend on previous research, showing that, in addition to the widely researched N, red fluorescence and the red to far-red peak ratio fluorescence peak ratio are able to track phosphorus, potassium, magnesium, sulfur, copper, manganese, and zinc in potato plants.

To visualize what effect the temporal variation had on the relationships between spectral indices and foliar nutrients, we analyzed the correlations separating the results by measuring point. This allowed us to identify those relationships that remained consistent over the whole measurement period (Study II, Figures 8 & 9), as well as those that presented contrasting patterns. These contrasting patterns would then indicate changes in the underlying physiological processes affecting the relationships. The relationships between leaf chlorophyll contents and red fluorescence, fluorescence peak ratio, MTCI, red edge reflectance and CCI remained constant between the early and late measurements. This same result could be noted for leaf nitrogen contents and the mentioned spectral indices, suggesting that the relationship of these spectral indices with N and leaf chlorophyll contents was not disturbed during the study period. Additionally, we identified results where the correlations were absent when investigating a single measuring point but appeared when pooling data from both points together. This would suggest an indirect effect mediating the relationship between nutrients and spectral indices, such as leaf morphology.

In Study III, to answer the need for long term, in situ measurements of photosynthesis regulation, we present a first demonstration of integrated PAM-ChlF and gas exchange measurements with the shoot chamber and MICRO-PAM systems. Through high temporal resolution measurements using the novel integrated instrument, this setup allowed us to simultaneously follow both the light and carbon reactions of photosynthesis and their dynamics in changing environmental conditions. Our study period encompassed the month of July in 2021 and included periods of high temperatures. During this period, we measured environmental conditions (PAR, temperature, precipitation), ChlF parameters (F, Fm', Y(II), ETR, F_v/F_m), as well as CO₂ assimilation (A_{NET}). The ChlF measurements were validated with concurrent MONI-PAM measurements. While the fluorescence parameters remained relatively stable during the period, a decreasing tendency could be noted in A_{NET} (Study III,

Figure 2 H), which was closely tied to a decreasing g_s . While A_{NET} was clearly affected by the heat periods and low water availability (Study III, Figure 2 H, Figure S2), fluorescence parameters were not affected to the same degree. ETR increased during the second heat period, but to a much lesser degree than A_{NET} and while the F_v/F_m parameter did not respond to low water availability or high temperature periods, it did decrease during cool nights between the two high temperature periods. Additionally, increased precipitation and lower temperatures after the second heat period led to a rapid increase in g_s and A_{NET} , (Study III, Figure 2 J, Figure 2 L). Furthermore, we calculated the ETR/A_{NET} parameter, which acts as an approximation for the number of electrons needed in the ETR for the assimilation of one CO_2 molecule. The ratio has a regular diurnal pattern (values changing between 3 – 20) during early July (Figure 4 inset). In this diurnal pattern, the ratio increases during the morning hours and only starts to decrease in the late afternoon. This cycle is linked to a decrease in g_s before noon, caused by increasing VPD and leading to decreasing A_{NET} values (Chaves, 1991), while the ETR remains relatively stable. However, during high temperature periods, the ratio exhibits large variations (Figure 5). These variations in the proxy values are caused by differing sensitivity of the ETR and A_{NET} reactions to environmental conditions (Perera-Castro & Flexas 2023), further detailed in the Discussion-section. Our high temporal resolution measurements, made possible by the new methodology brought forward in Study III, allowed for the recording of the ETR/A_{NET} in situ, over a long period of time.

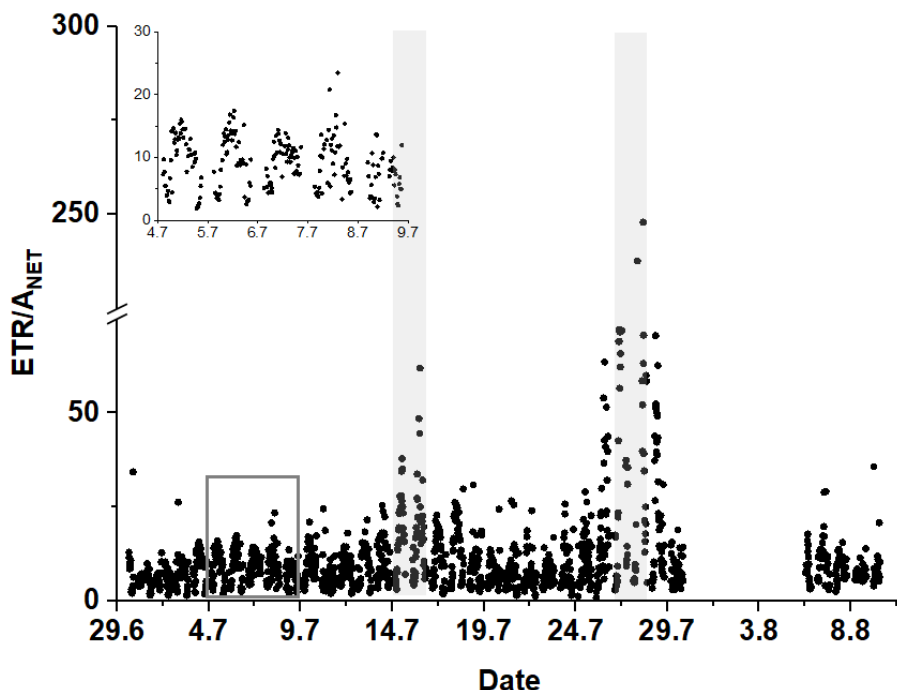


Figure 5 The ETR/A_{NET} ratio from Study III, calculated as the ratio between electron transport rate (ETR) and net photosynthetic assimilation (A_{NET}). Black dots indicate individual measurements, while high temperature periods are marked with grey bars. To further clarify the diurnal variation of the ratio, an inset has been added to the top left corner. This inset zooms in on the period between 4.7 – 9.7 and is marked by a grey box in the main figure. To improve readability of the figure, a break has been added to the y- axis of the main figure. Figure adapted from Study III.

4.2 Variables affecting the scaling of leaf spectral signals from the leaf to the canopy

When scaling leaf spectral signals to the canopy level, the signal is always affected by various factors, such as viewing geometry and canopy structural variables. For this reason, it is of utmost importance to be able to understand and quantify the processes that decouple the leaf level signal from the canopy level signal, such as leaf area index (LAI), fractional vegetation cover (FVC), LAD and, in SIF measurements, the escape probability of ChlF (f_{esc}) (Zeng et al. 2019). One way of investigating the changes that a variable scale brings is to conduct simultaneous measurements on the leaf and canopy scales.

In Study I, we performed UAV and leaf level measurements to investigate how water stress caused changes in photosynthetic and canopy structural parameters on both the diurnal and longer (two-week measurement period) time scales. From our results comparing water stressed treatment plots to the control plots after the two-week measuring period, we notice that water stress induced differences in both photosynthetic and canopy structural variables (Study I, Figure 4). The water stressed plots had lower LAI (1.78 versus 2.22), higher average leaf angle (ALA) (57.9° versus 55.2°) and higher leaf chlorophyll contents (49.4 versus 42.2

$\mu\text{g}/\text{cm}^2$) than the control plots. Higher ALA consequently affected the relative contribution that LAD had on the SIF signal. In measurements accounting for the whole two-week study period, the water stress was mainly expressed as changes in LAI (affecting APAR) between plots (explaining 20 – 72 % of variability between treatments), as well as changes in f_{esc} , caused by LAD dynamics, contributing 5 – 39 % of variation (Study I, Figure 9). This analysis showed that a decrease in far-red ChlF emission could be observed as a response to water stress both in simulated and observed SIF.

Additionally, a sensitivity analysis was performed on a water stress treatment and control plot pair to assess which factors were the main drivers of diurnal differences in SIF. We found that, on the diurnal scale, the differences between SIF emission in the treatment and control plots were driven by variation in APAR (which was affected by leaf chlorophyll and LAI, explaining 39% of the difference in SIF), Φ_{F_PSII} (explaining 30-36 % of differences) and LAD variation (explaining 25 – 31 %, most of it due to changes in f_{esc} (22 – 28 %)). In other words, the diurnal variation of SIF emission between the control and treatment plots was driven both by canopy structural and photosynthetic variables. It is important to note that for non-woody plants, the diurnal changes of LAD have the potential to be an important source of misinterpretation of dynamics in remote sensing data, if static vegetation architecture is assumed, as changes in f_{esc} could be then interpreted as changes in the photosynthetic physiology of the leaves (Study I).

In Study II, we used reflectance based vegetation indices combined with ChlF measurements to detect leaf nutrient contents variations at both temporal and spatial scales. Temporal variation was accounted for by using two different measuring points with 20 days in separation. In addition to spectral remote sensing measurements, we calculated a fractional vegetation cover (FVC)-variable to estimate the effect of the developing canopy to the relationship between spectral measurements and leaf nutrients during the measurement period. This variable, estimated from the multispectral imaging data we collected from the UAV, was calculated for all of the treatments separately and we noticed a non-significant increase in FVC during the study for all treatments except the water stressed one. This use of multispectral data allowed the estimation of canopy structural parameters directly from remote sensing measurements. As the FVC was used as a proxy for canopy development, its relationship with each vegetation index and ChlF emission at the canopy scale was calculated. Interestingly, far-red fluorescence, red edge reflectance, CCI and NDVI were the only spectral indices with relatively high Pearson correlation ($R > 0.60$) with FVC, none of which were correlated with foliar chlorophyll levels at the canopy scale.

The relationships between foliar nutrients and canopy level spectral indices differed from those at the leaf level. Both the red fluorescence and fluorescence peak ratio were positively correlated with Group 1 nutrients, while being negatively correlated with Group 2 nutrients (Figure 5). PRI, on the other hand, had weak positive correlation with Group 1 nutrients and strong negative ones with Group 2 nutrients. Additionally, red fluorescence, fluorescence peak ratio and PRI were negatively correlated with the Car/Cab ratio at the canopy level. Furthermore, it should be noted that in the correlations between foliar nutrients and fluorescence parameters, the relationships were inverted when moving from the leaf to the canopy scale. In other words, relationships that were positive on the leaf level were negative on the canopy level, and vice versa.

In addition to investigating pooled results from both measuring points in Study II (as shown in Figure 4), we additionally separated the results by measuring point to examine the role of temporal changes on the relationships between foliar nutrient contents and spectral indices (Figures 8 & 9, Study II). Unlike in the leaf level results, only the relationship between

CCI and nitrogen was found to be consistent over time. In other words, only in this case did the relationship between nutrient and spectral signal remain the same on both individual measuring points and when pooling all the data together. In the other canopy level relationships, while the spectral indices correlated with the nutrients when looking at the pooled data, the relationships in individual measurement points were affected by additional factors, breaking said relationships. The most important of these factors would most likely be the varying canopy structure, which would naturally not be a factor in leaf level results. In general, stronger correlations between canopy spectral signals and leaf nutrients could be noted in the second measuring point relative to the first one, possibly caused by enhanced variability due to nutrient and water stress treatments having an impact on leaf and canopy development. Finally, some correlations between spectral signals and leaf nutrients only emerged when the data was pooled together across both measuring points, such as between fluorescence peak ratio and phosphorus. These findings emphasize the role of canopy development as the mediator in the relationship between spectral remote sensing and leaf nutrients at the canopy scale.

5. DISCUSSION

The proliferation of remote sensing measurements of vegetation at the end of the 20th century and the beginning of the 21st century has opened up new possibilities for the cost-effective and timely collection of data, aiding in the characterization of plant stress responses and photosynthesis research at scale (Zarco-Tejada et al. 2012; He et al. 2020). These measurements have been made possible by advances in both remote sensing platform and sensor technology (de Castro et al. 2021). Early vegetation indices were based on the differences on reflectance and absorbance characteristics of vegetation in the visible and infrared regions (Jordan, 1969; Rouse et al. 1974). The availability of hyperspectral remote sensing coupled with advancements in SIF retrieval and processing has meant that new information related to crop stress (Lassalle, 2021), water content (Zhang & Zhou, 2018) and gross primary productivity (GPP) (Sun et al. 2017) is now available. In order to obtain precise information from the measured object, novel methods are required to quantify the effects that scale, and the underlying leaf level mechanisms have on the remote sensing signal.

Through the implementation of novel UAV-based methods to assess canopy structural variables, as well as new instrumentation integrating both optical and gas exchange measurements into a single system this thesis aimed to present novel methods for facilitating the mechanistic interpretation of multiscale optical remote sensing measurements. The results provided in the three studies included in this thesis lay out promising developments in remote sensing signal interpretation. In the following section, these results are viewed in the context of i) interpretation of the underlying mechanistic ecophysiological processes that affect the signal at the leaf level, and ii) interpreting canopy level remote sensing signals as they are scaled from leaf to canopy.

5.1 Co-registration of leaf physiological processes and spectral signals

SIF and GPP are well known to be correlated at diverse scales (Damm et al. 2015; Sun et al. 2018; Magney et al. 2019). As such, Study I concentrated on revealing the interplay between variations in structure and photosynthetic physiology that couple and decouple this connection under water stress, something that has yet to be quantified in previous research. The results from Study I point to the dynamics of fluorescence yield between stressed and non-stressed plots to be in line with earlier research, since as can be observed from Figure 10 in Study I, the plots suffering from water stress had lower fluorescence yield when compared to the control plots. This is due to limited water uptake causing stomatal closure, which in turn leads to a decrease in intercellular CO₂ concentration (Farquhar et al. 1980, Cornic, 2000), while also reducing the carbon assimilation rate and affecting the partitioning of carboxylation / oxygenation of RuBisCO to favor photorespiration (Flexas et al. 2000). In addition, stomatal closure reduces carbon assimilation, which leads to a decrease in fluorescence yield and LUE due to increased NPQ (Flexas et al. 2000). The effect that these leaf level processes, together with processes on the canopy level, have on the relationship between SIF and GPP is discussed in more detail in Section 5.2.

In Study II, the relationships between multiscale measurements of ChlF and reflectance based spectral indices and a wide range of micro- and macronutrients was investigated for the first time. Reflectance based vegetation indices are affected by leaf morphology, canopy structure and the pigment pools in the leaves, the latter of which can vary due to stress, such as nutrient deficiency (Ögren, 1988, Hashmi et al. 2019). As such, we hypothesized that spectral indices related to photoprotection (PRI, CCI), as well as ChlF, through their direct connection with the leaf physiological processes, would be more strongly related to leaf nutrient levels than more traditional greenness-based indices. The results from Study II support this hypothesis.

A temporal division of nutrients during the study period into two distinct groups could be noticed, where Group 1 nutrients all decreased during the measurement period, while Group 2 nutrients increased. This division is most likely caused by the so-called dilution phenomenon (Lambers & Oliveira, 2019), where the increased use of macronutrients causes a decrease in foliar nutrient contents over the growing season (Abukmeil et al. 2022). While Group 2 nutrients were negatively correlated with leaf chlorophyll, Group 1 nutrients were positively correlated with leaf chlorophyll amounts, indicating that the allocation of these nutrients into chlorophyll synthesis was not disrupted by drought or nutrient variation during the study period.

While red fluorescence emission and fluorescence peak ratio, in addition to CCI, red edge reflectance and MTCI were all correlated with Group 1 nutrients (nitrogen, phosphorus, potassium and magnesium), NDVI was not. As such, the NDVI signal has been found to saturate in high leaf chlorophyll conditions, which was also the case in our study (Gitelson et al. 1996; Satognon et al. 2021). The connection between MTCI, red edge reflectance and the nutrients was through their coupling to the leaf chlorophyll amounts: increasing chlorophyll amounts in the leaf shifts the red edge feature towards higher wavelengths (Filella & Peñuelas, 1994), causing it to be less susceptible to saturation than the red reflectance band (Kanke et al. 2012). The carotenoid / chlorophyll – ratio (Car/Cab) provides information about the physiological status of the plant. As plants suffer from stress, the amount of protective pigments increases in relation to chlorophyll, increasing the Car/Cab ratio. The photoprotection-related indices PRI and CCI were expected to be inversely related to photoprotection, as they are sensitive to the carotenoid – chlorophyll ratio (Car/Cab)

(Gamon et al. 1992; Filella et al. 2009). In other words, PRI and CCI should decrease when leaves have increased levels of protective carotenoids. In our study, only PRI was negatively correlated with the Car/Cab ratio, while CCI was negatively correlated with leaf chlorophyll amounts. This would indicate that in our study, while PRI was driven by changes in carotenoids, changes in CCI were driven by leaf chlorophyll amounts at the leaf level, explaining their different correlations to leaf nutrients.

Finally, the negative correlation between Group 1 nutrients and red ChlF, as well as ChlF peak ratio could be explained by the re-absorption of red fluorescence by chlorophyll inside the leaf (Buschmann, 2007, Romero et al. 2018). When a leaf has low chlorophyll contents, an increase in chlorophyll level leads to an increase in APAR and thus the ChlF emission. However, at high chlorophyll contents, such as in our study, an increase in the chlorophyll contents of the leaf increases re-absorption to a much higher degree than APAR due to self-shading within the leaf (Study I, Buschmann, 2007). The dynamics of re-absorption would explain i) the strong relationships between red ChlF and ChlF peak ratio and ii) the lack of correlations between far-red ChlF emission and leaf chlorophyll contents (and by extension the nutrients tied to leaf chlorophyll level).

To conclude, at the leaf level, the perceived correlations between leaf nutrients and spectral indices are driven by leaf chlorophyll (MTCI, red edge, CCI) and carotenoid (PRI) dynamics, as well as the interplay between leaf chlorophyll and chlorophyll re-absorption (fluorescence parameters).

In Study III, in order to investigate the dynamics of light and carbon reactions of photosynthesis with high temporal resolution measurements, we followed ChlF and gas exchange parameters for a period of one month. During the study, we noticed that stomatal conductance (g_s) and net carbon assimilation had a decreasing tendency, caused by decreasing water availability and high temperatures. Our results from the ChlF and gas exchange measurements were encapsulated in the ETR/A_{NET} – ratio, which indicates the number of electrons needed for the assimilation of one CO_2 molecule. This ratio has been shown to be increased by several factors, such as photorespiration, mitochondrial respiration, and alternative energy sinks, which affect the rate of electron transport (Alric and Johnson, 2017; Alboresi et al. 2019; Walker et al. 2020). Earlier research has shown the carbon assimilation process to be more sensitive to drought conditions than the PSII machinery (Flexas et al. 2002). Additionally, several factors help maintain PSII activity in low water availability conditions. This includes increased photorespiration, as well as the Mehler reaction (Flexas et al. 2007) and alternative energy sinks (Flexas et al. 2000; Sunil et al. 2019; Perera-Castro & Flexas, 2023). The combination of these factors, in addition to increased mesophyll conductance, are potentially causing very high ETR/A_{NET} values during high temperature periods in our study. The precise detection of these changes in the ETR/A_{NET} ratio is made possible by the high temporal resolution in situ measurements presented for the first time in Study III (Figure 4). The ETR/A_{NET} ratio has been shown to be a good indicator for plant stress (Flexas et al. 2002; D'Ambrosio et al. 2006) and in our study seems to be responding to periods of low water availability and high temperatures.

However, since some assumptions are required for the ETR calculation, the validity of these assumptions across differing environmental conditions and species should be revisited. This includes the constant value of 0.84 for leaf absorption, which can be a potential source of error in ETR calculations (Blache et al. 2011). Also, the partitioning of energy between photosystem I (PSI) and PSII is assumed to be a constant 0.5 (Krall and Edwards, 1992; Laik & Loreto, 1996), which could provide an error in ETR calculation. This error could be caused by the uneven amount of PSI and PSII reaction centers (Anderson et al. 1988), as well as the

differences in pigment composition and absorbance spectra between the photosystems (McClain and Sharkey, 2020), causing changes in energy partitioning between photosystems. Finally, while often neglected, the PSI contribution to the quantum yield of photochemistry should be taken into account in ETR calculations. Previous work by Pfündel (1998), Agati et al. (2000) and Franck et al. (2002) suggest that PSI could be an important contributor to F , but not F_M , affecting ETR calculations. To conclude, the results from Study III present a clear methodological advance in photosynthesis research. While we are able to successfully track the seasonal regulation of photosynthesis in silver birch with our novel setup, further improvements could be made. The improvements could be carried out by implementing an integrated spectrometer, allowing for better estimation of APAR and energy partitioning within the leaf, linking the results to reflectance based spectral indices and spectral fluorescence. Further measurements with similar setups would potentially lead to advances in photosynthesis modelling and interpretation of remote sensing data.

The first aim of this thesis was to quantify the physiological processes that connect spectral measurements to photosynthesis and nutrient contents at the leaf level. In Study III, the long-term interplay of physiological processes and spectral signals was investigated *in situ* for the first time using a novel instrument setup. The integrated high temporal resolution measurements of ChlF and gas exchange allowed for the investigation of photosynthesis downregulation, possibly leading to advances in photosynthesis remote sensing and modelling in the future. The leaf level physiological effects of water stress were investigated in Study I. We found that water stress decreased leaf stomatal conductance, increasing leaf photorespiration, leading to a decrease in SIF emission. With the quantification of these leaf level physiological measurements, we are able to investigate the relative effect that these processes have on the SIF – GPP relationship, along with canopy structural variables. Study II concentrated on the factors driving the relationship between leaf nutrient contents and spectral signals, while investigating a wide array of micro- and macronutrients. The results from the combined multiscale measurements point to leaf pigments being the main drivers of these relationships at the leaf level and call for multisource measurements to quantify the physiological processes causing changes in leaf level spectral indices.

5.2 Impacts of canopy structural effects on the scaling of the remote sensing signal from leaf to canopy

The second goal of this thesis was to investigate the spatial factors that affect the spectral remote sensing of photosynthesis and leaf nutrients when the signal is scaled from the leaf to the canopy. Consequently, Study I investigated how water stress affects the relationship between canopy structure, photosynthetic factors and SIF. On the diurnal scale, water stress was found to induce changes in canopy structure by increasing ALA. The higher ALA in water stressed plots, especially around noon, would point to a loss of turgor, causing the plants to close their stomata to preserve water, leading to reduced transpiration rates (Reynolds-Henne et al. 2010; Obidiegwu et al. 2015). This noon wilting has been commonly noted in non-woody crops and also causes changes in LAD (Xu et al. 2018). Additionally, we observed an increase in ALA during the morning hours, which started to decrease towards the evening (Study I, Figure 5 F) in both the water stressed and control plots, with these changes being comparably more drastic in the water stressed plots. Surprisingly, the water stressed plots had higher leaf chlorophyll amounts, which would most likely point to nutrient relocation within plants to top leaves, as has been noted earlier with plants in water limited

conditions (Munné-Bosch & Alegre, 2004, Study II). Furthermore, due to the water stress induced changes in canopy structure (LAD, LAI, f_{esc}) and reductions in fluorescence quantum efficiency (Φ_F), a clear reduction in the SIF signal could be noted when comparing the water stressed plots to the control plots on the diurnal scale. Based on our measurement results, combined with the simulation results, we conclude that both LAD and Φ_F are as important as drivers of SIF response to water stress on a diurnal scale.

In addition to diurnal variation, our study investigated the effects that water stress has on the SIF-GPP relationship as the stress affects the photosynthetic and structural variation of the canopy over a two-week measuring period. Over this period, the relationship between SIF and GPP is mediated by both structural and physiological factors, with APAR (changes in which are driven by LAI and leaf chlorophyll contents), Φ_{F_PSII} and LAD being the most important factors. We conclude that the response of SIF to water stress is caused by a multitude of factors, which are a combination of both physiological and structural variables. Some of the changes in SIF emission that are caused by structural factors could therefore be misconstrued as being caused by changes in Φ_F . Furthermore, some differences have been found in the SIF response to water stress between earlier experimental results (Helm et al. 2020) and satellite observations (Magney et al. 2020; Sun et al. 2015). As structural effects affect the remote sensing signal differently depending on the scale of observation, novel UAV-based observations of SIF and structural properties, such as presented in Study I, could help bridge the gap between experimental results and satellite-level observations.

One of the objectives of Study I was to characterize the mechanisms that drive the spatial response of SIF in water stressed potato plants. We found that structural dynamics, foremost being LAD had an important role in modulating SIF variation. Additionally, we were interested in finding out how these mechanisms affected the SIF – GPP dynamic. As shown in Eq. 3, in an ideal situation, the relationship between SIF and GPP depends on the variation of light use efficiency (LUE), Φ_F and f_{esc} . This relationship is however affected by plant stress responses, such as changes in the photochemistry in the form of increased photorespiration, and in changes to the plant structure in the form of changing leaf angles. Therefore, the relationship between SIF and GPP in water stressed conditions is modulated by photochemistry through LUE, fluorescence yield and f_{esc} , as well as canopy structure through changes in leaf angle distribution (Figure 6). The results from Study I simulations would additionally point to canopy structural elements coupling SIF and GPP together, rather than acting as a decoupling factor. This is shown by the simulated relationships between SIF and GPP improving when accounting for changes in LAD and fluorescence yield. Results from Study I show that the separation of canopy structural effects from the underlying signal

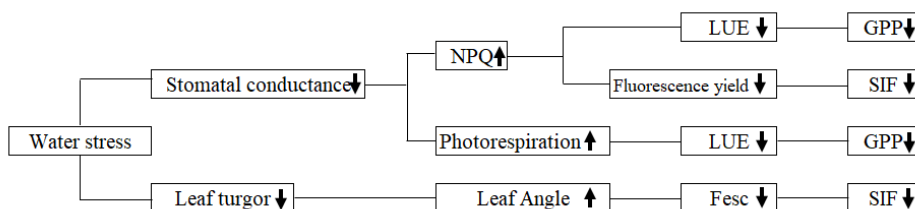


Figure 6 Schematic of the responses of SIF and GPP to water stress through decreasing leaf turgor and stomatal conductance. Importantly, both of these effects separately decouple SIF and GPP, but our results point to them cancelling each other out. Figure adapted from Study I.

originating from the photosynthetic processes can be difficult to discern without the use of multiscale measurements.

Based on the results from Study I, we conclude that on the diurnal scale, SIF responded to fluorescence quantum efficiency and LAD, while on the longer temporal scale variation in SIF was mostly modulated by structural factors. Thus, while the SIF emission decreased during the study, this decrease in SIF signal during the water stress period could not be attributed to a single driver but was caused by a combination of structural and physiological factors. Consequently, in future research, we advocate for concurrent field and remote sensing measurements to further our quantitative understanding of the interaction between SIF and canopy structural parameters.

While spectral indices were found to be correlated with many nutrients at the leaf level in Study II, most of the relationships between spectral indices and leaf nutrient contents broke down when moving to the canopy scale spectral measurements. Additionally, at the canopy scale, the correlations between nutrient groups and spectral indices presented inverted patterns (red fluorescence), decreased considerably (red edge reflectance and MTCI), increased (PRI) or remained similar in the case of CCI. Our results are not in line with earlier research showing that MTCI was able to track leaf N concentrations (Nigon et al. 2015) in potato. This could in part be due to differences in canopy structure between the studies and the susceptibility of red edge based VI's to the impact of bare soil (Li et al. 2014). The distinctly different patterns between scales clearly indicate that, in the case of our fertilization and water stress treatments, the leaf level spectral signals are greatly affected by canopy structural variables when scaled to the canopy level. From the results of leaf nutrient contents and their relationships with canopy level ChlF and greenness- and photoprotection-related vegetation indices in Study II, we conclude that the relationship between foliar nutrients and greenness-based indices seems to depend on the spatiotemporal co-variation of canopy development (here parametrized in FVC) and leaf chlorophyll contents, which in our case was very limited. This would be supported by the lower correlations between greenness-based indices and foliar nutrients during the first measurement point (Study II, Figure A12).

Canopy scale ChlF emission is driven by changes in the amount, arrangement and angles of the leaves in the canopy, affecting APAR, fesc and ChlF-reabsorption (Study I; Liu et al. 2019; Verrelst et al. 2015). Increased chlorophyll levels in leaves lead to a rise in APAR, which consequently increases the ChlF emission of the leaf. However, the increase in leaf chlorophyll also increases the chance of ChlF re-absorption, which primarily affects the red fluorescence emission. The concentration of the chlorophyll molecules within the leaf dictates the level at which the increase in re-absorption overtakes the increase in ChlF emission (Liu et al. 2019). As canopy level red fluorescence emission was weakly positively correlated with FVC, it would indicate that the APAR effect still dominated over the re-absorption effect on the canopy scale. Additionally, the fact that far-red ChlF was positively correlated with FVC would indicate that the effect of LAI on canopy APAR was not yet saturated and a higher FVC would still increase far-red ChlF emission (Zhang et al. 2016). Furthermore, the strong and positive relationship between far-red fluorescence and FVC seems to point to the importance of canopy structural dynamics as a driver of ChlF dynamics at the canopy scale (Study I; Chang et al. 2021).

Foliar nutrient contents were not dependent on canopy cover, which was further emphasized by the lack of correlations of far-red ChlF with any of the nutrients. Also, as both red ChlF and ChlF peak ratio are sensitive to both APAR and reabsorption dynamics, they would appear to have an enhanced capability to track foliar nutrients over far-red ChlF.

In Studies I & II, the effects of spatial change on the remote sensing signal was explored. In Study I, to help interpret and model the connections between SIF and GPP, we aimed to disentangle the effects of photosynthetic and structural dynamics on the SIF – GPP relationship. We noted that the LAD was one of the main drivers in the relationship between SIF and GPP on the diurnal and longer time scales. Furthermore, we conferred that water stress caused changes in LAI and f_{esc} in addition to LAD, all of which affected the relationship between GPP and SIF on a diurnal scale. As Study I gave insight into the physiological and canopy structural response to water stress, we conclude that leaf angular variation should be taken into account when investigating the relationship between SIF and canopy structure. In Studies I & II, the canopy level spectral measurements were conducted from a UAV, which provided a flexible and low-cost solution for canopy level spectral measurements. As such, UAV-based spectral measurements could in the future help narrow the gap between leaf and satellite level observations. In Study II, we provided leaf scale measurements of numerous micro- and macronutrients, combined with multi-scale measurements of spectral signals. While the relationships between foliar nutrient contents and spectral signals were driven at the leaf level by leaf chlorophyll concentration, on the canopy level the relationships were modulated by a combination of chlorophyll concentration and structural properties. The capacity of spectral signals to detect leaf nutrients thus depended on covariation between nutrients, canopy structure and leaf pigments. As such, to be capable of scaling leaf nutrients to canopy level measurements, these factors should be taken into account in future measurements. To resolve the spatial and temporal dynamics of leaf nutrients from the canopy scale, we propose that novel imaging solutions combined with modern radiative transfer models would be utilized in the future (Lu et al. 2020; Ye et al. 2020).

Both Studies I & II relied on simultaneous measurements conducted on both leaf and canopy levels, allowing for the complementary information provided by several scales, making the quantification of the effects caused by scaling possible. The results from Studies I & II into the effects of variable spatial scale affecting the leaf level signal provide insights to the interpretation of remote sensing signals discussed in Sections 1.4 & 1.5.

6. CONCLUSIONS

Via the development and validation of novel methods and instruments, this thesis contributes to the interpretation of multiscale optical remote sensing of nutrients and photosynthesis. These novel methods are here used to quantify the i) connections between leaf spectral signals and physiological processes, as these processes are affected by regulatory mechanisms in a temporal dimension, ii) spatial factors that affect the spectral remote sensing signal when scaling the signal from leaf to canopy scale.

In Study I, we found different drivers for the SIF response to water stress on the diurnal and longer temporal scales. Additionally, we presented the potential of UAV-based SIF and hyperspectral measurements to detect changes in canopy structural variables, such as LAD and LAI, and how these changes affected the SIF emission as well as the SIF – GPP relationship. We conclude that the focus of the relationship between canopy structure and SIF should, using data from multiple sources or scales, additionally take into account leaf

angular variation on the diurnal and spatial scales. Finally, the versatility of UAV's could help bridge the gap between field and satellite measurements.

In Study II, UAV-based remote sensing measurements were used to estimate changes in canopy structure in the form of FVC, validated by its high correlation with several canopy level spectral indices. Canopy level spectral measurements of leaf nutrient contents were found to depend on the spatiotemporal covariation of nutrients, chlorophyll and canopy structure. Thus, we conclude that novel imaging or multi-angle measurements, combined with 3D radiative transfer methods would be needed to develop novel methods for the estimation of leaf nutrient contents from the canopy scale.

We demonstrated the potential of integrated, continuous and long-term measurements of ChlF and gas exchange in Study III. This new instrument setup, conducting continuous high temporal resolution field measurements, opens new possibilities to look into the drivers of photosynthetic downregulation, offering opportunities in photosynthesis modelling, remote sensing and field research.

To conclude, the novel methods and instrumentation presented in this thesis lay the groundwork for better quantification of canopy structural parameters, as well as photosynthesis downregulation dynamics, allowing for advances in the remote sensing of photosynthesis and nutrients. This thesis calls for implementation of new instrumentation and methodologies that can be used to co-register spectral and physiological variables at multiple scales simultaneously. These multiscale measurements will be key in connecting spectral signals to leaf physiological processes across scales. Additionally, to advance the interpretation of the processes that connect ChlF with photosynthesis, the novel instrument combining ChlF and gas exchange measurements could in the future be improved with a spectrometer, opening new possibilities for the estimation of energy partitioning within the leaf, advancing photosynthesis modelling and interpretation of remote sensing data. Finally, I see potential in combining multi-scale high spatial resolution observations coupled to advanced 3D radiative transfer models, machine learning methods and fluorescence-based imaging systems in helping resolve questions related to spatial variability of plant regulatory and control processes.

REFERENCES

Aasen, H, Van Wittenberghe, S, Sabater Medina, N, Damm, A, Goulas, Y, Wieneke, S, Hueni, A, Malenovský, Z, Alonso, L, Pacheco-Labrador, J, Cendrero-Mateo, MP (2019) Sun-induced chlorophyll fluorescence II: Review of passive measurement setups, protocols, and their application at the leaf to canopy level. *Remote Sens* 11(8): 927. <https://doi.org/10.3390/rs11080927>

Abadía, J (1992) Leaf responses to Fe deficiency: a review. *J Plant Nutr* 15(10): 1699–1713. <https://doi.org/10.1080/01904169209364432>

Abukmeil, R, Al-Mallahi, AA, Campelo, F (2022) New approach to estimate macro and micronutrients in potato plants based on foliar spectral reflectance. *Comput Electron Agric* 198: 107074. <https://doi.org/10.1016/j.compag.2022.107074>

Ač, A, Malenovský, Z, Olejníčková, J, Gallé, A, Rascher, U, Mohammed, G (2015) Meta-analysis assessing potential of steady-state chlorophyll fluorescence for remote sensing detection of plant water, temperature and nitrogen stress. *Remote Sens Environ* 168: 420–436. <https://doi.org/10.1016/j.rse.2015.07.022>

Adams III, WW, Demmig-Adams, B (1992) Operation of the xanthophyll cycle in higher plants in response to diurnal changes in incident sunlight. *Planta* 186(3): 390–398. <https://doi.org/10.1007/BF00195320>

Adams III, WW, Winter, K, Schreiber, U, Schramel, P (1990) Photosynthesis and chlorophyll fluorescence characteristics in relationship to changes in pigment and element composition of leaves of *Platanus occidentalis* L. during autumnal leaf senescence. *Plant Physiol* 92(4): 1184–1190. <https://doi.org/10.1104/pp.92.4.1184>

Agati, G., Fusi, F., Mazzinghi, P., & di Paola, M. L. (1993). A simple approach to the evaluation of the reabsorption of chlorophyll fluorescence spectra in intact leaves. *J Photoch Photobio B* 17(2): 163–171. [https://doi.org/10.1016/1011-1344\(93\)80009-X](https://doi.org/10.1016/1011-1344(93)80009-X)

Agati, G, Mazzinghi, P, Fusi, F, Ambrosini, I (1995) The F685/F730 chlorophyll fluorescence ratio as a tool in plant physiology: response to physiological and environmental factors. *J Plant Physiol* 145(3): 228–238. [https://doi.org/10.1016/S0176-1617\(11\)81882-1](https://doi.org/10.1016/S0176-1617(11)81882-1)

Agati, G, Cerovic, ZG, Moya, I (2000) The effect of decreasing temperature up to chilling values on the in vivo F685/F735 chlorophyll fluorescence ratio in *Phaseolus vulgaris* and *Pisum sativum*: the role of the photosystem I contribution to the 735 nm fluorescence band. *Photochem Photobiol* 72(1): 75–84. [https://doi.org/10.1562/0031-8655\(2000\)0720075TEODTU2.0.CO2](https://doi.org/10.1562/0031-8655(2000)0720075TEODTU2.0.CO2)

Agati, G, Foschi, L, Grossi, N, Guglielminetti, L, Cerovic, ZG, Volterrani, M (2013) Fluorescence-based versus reflectance proximal sensing of nitrogen content in *Paspalum vaginatum* and *Zoysia matrella* turfgrasses. *Eur J Agron* 45: 39–51. <https://doi.org/10.1016/j.eja.2012.10.011>

Al Suwaidi, A (2012) DubaiSat-2 mission overview. *Proc Spie* 8533: 220–224. <https://doi.org/10.1117/12.974469>

Alboresi A, Storti M, Morosinotto T (2019) Balancing protection and efficiency in the regulation of photosynthetic electron transport across plant evolution. *New Phytol* 221(1): 105–109. <https://doi.org/10.1111/nph.15372>

Alric J, Johnson X (2017) Alternative electron transport pathways in photosynthesis: a confluence of regulation. *Curr Opin Plant Biol* 37: 78–86. <https://doi.org/10.1016/j.pbi.2017.03.014>

Ananyev, G, Kolber, ZS, Klimov, D, Falkowski, PG, Berry, JA, Rascher, U, Martin, R Osmond, B (2005) Remote sensing of heterogeneity in photosynthetic efficiency, electron transport and dissipation of excess light in *Populus deltoides* stands under ambient and elevated CO₂ concentrations, and in a tropical forest canopy, using a new laser-induced fluorescence transient device. *Glob Change Biol* 11(8): 1195–1206. <https://doi.org/10.1111/j.1365-2486.2005.00988.x>

Anderson, JM, Chow, WS, Goodchild, DJ (1988) Thylakoid membrane organisation in sun/shade acclimation. *Plant Biol* 15(2): 11–26. <https://doi.org/10.1071/PP9880011>

Arena, C, Vitale, L, De Santo, AV (2008) Paraheliotropism in *Robinia pseudoacacia* L: an efficient strategy to optimise photosynthetic performance under natural environmental conditions. *Plant Biol* 10(2): 194–201. <https://doi.org/10.1111/j.1438-8677.2008.00032.x>

Asner, GP, Wessman, CA, Archer, S (1998) Scale dependence of absorption of photosynthetically active radiation in terrestrial ecosystems. *Ecol Appl* 8(4): 1003–1021. [https://doi.org/10.1890/1051-0761\(1998\)008\[1003:SDOAO\]2.0.CO;2](https://doi.org/10.1890/1051-0761(1998)008[1003:SDOAO]2.0.CO;2)

Atherton, J, MacArthur, A, Hakala, T, Maseyk, K, Robinson, I, Liu, W, Honkavaara, E, Porcar-Castell, A (2018) Drone measurements of solar-induced chlorophyll fluorescence acquired with a low-weight DFOV spectrometer system. *IGARSS 2018–2018 Int Geosci Remote Se*: 8834–8836. <https://doi.org/10.1109/IGARSS.2018.8517474>

Atherton, J, Liu, W, Porcar-Castell, A (2019a) Nocturnal Light Emitting Diode Induced Fluorescence (LEDIF): A new technique to measure the chlorophyll a fluorescence emission spectral distribution of plant canopies in situ. *Remote Sens Environ* 231: 111137. <https://doi.org/10.1016/j.rse.2019.03.030>

Atherton, J, Xu, S, Porcar-Castell, A (2019b) Heuristic methods to correct for wavelength offset effects in dual field of view spectrometer systems. In: *Proceedings of the Center of Excellence in Atmospheric Science (CoE ATM) Annual Seminar 2019 Finnish Association for Aerosol Research FAAR*: 169–171.

Aubinet, M, Vesala, T, Papale, D (Eds) (2012) *Eddy covariance: a practical guide to measurement and data analysis*. Springer Science & Business Media. <https://doi.org/10.1007/978-94-0072351-1>

Bailey, BN, Kent, ER (2021) On the resolution requirements for accurately representing interactions between plant canopy structure and function in three-dimensional leaf-resolving models in silico. *Plants*: 3(2). <https://doi.org/10.1093/insilicoplants/diab023>

Baker, NR (2008) Chlorophyll fluorescence: a probe of photosynthesis in vivo. *Annu Rev Plant Biol* 59: 89–113. <https://doi.org/89–113.10.1146/annurev.arplant.59.032607.092759>

Ball, JT, Woodrow, IE, Berry, JA (1987) A model predicting stomatal conductance and its contribution to the control of photosynthesis under different environmental conditions. *Progress in photosynthesis research: volume 4 proceedings of the VIIth international congress on photosynthesis*. Providence, Rhode Island, USA, august 10–15, 1986: 221–224 Dordrecht: Springer Netherlands. https://doi.org/10.1007/978-94-017-0519-6_48

Barton, CVM, North, PRJ (2001) Remote sensing of canopy light use efficiency using the photochemical reflectance index: Model and sensitivity analysis. *Remote Sens Environ* 78(3): 264–273. [https://doi.org/10.1016/S0034-4257\(01\)00224-3](https://doi.org/10.1016/S0034-4257(01)00224-3)

Berger, S, Benediktyová, Z, Matouš, K, Bonfig, K, Mueller, MJ, Nedbal, L, Roitsch, T (2007) Visualization of dynamics of plant–pathogen interaction by novel combination of chlorophyll fluorescence imaging and statistical analysis: differential effects of virulent and avirulent strains of *P syringae* and of oxylipins on *A thaliana*. *J Exp Bot* 58(4): 797–806. <https://doi.org/10.1093/jxb/erl208>

Blache, U, Jakob, T, Su, W, Wilhelm, C (2011) The impact of cell-specific absorption properties on the correlation of electron transport rates measured by chlorophyll fluorescence and photosynthetic oxygen production in planktonic algae. *Plant Physiol Bioch* 49(8): 801–808. <https://doi.org/10.1016/j.plaphy.2011.04.010>

Boyd, DS, Almond, S, Dash, J, Curran, PJ, Hill, RA (2011) Phenology of vegetation in Southern England from Envisat MERIS terrestrial chlorophyll index (MTCI) data. *Int J Remote Sens* 32(23): 8421–8447. <https://doi.org/10.1080/01431161.2010.542194>

Bremner, JM (1996) Nitrogen-total Methods of soil analysis: Part 3. *Chemical methods* 5: 1085–1121. <https://doi.org/10.2136/sssabookser5.3.c37>

Bronson, KF, White, JW, Conley, MM, Hunsaker, DJ, Thorp, KR, French, AN, Mackey, BE, Holland, KH (2017) Active optical sensors in irrigated durum wheat: Nitrogen and water effects. *Agron J* 109(3): 1060–1071. <https://doi.org/10.2134/agronj2016.07.0390>

Brugnoli, E, Björkman, O (1992) Chloroplast movements in leaves: influence on chlorophyll fluorescence and measurements of light-induced absorbance changes related to Δ pH and zeaxanthin formation. *Photosynth Res* 32: 23–35. <https://doi.org/10.1007/BF00028795>

Buschmann, C (2007) Variability and application of the chlorophyll fluorescence emission ratio red/far-red of leaves. *Photosynth Res* 92: 261–271. <https://doi.org/10.1007/s11120-007-9187-8>

Butler, WL (1978) Energy distribution in the photochemical apparatus of photosynthesis. *Ann Rev Plant Physio* 29(1): 345–378. <https://doi.org/10.1146/annurev.pp.29.060178.002021>

Camino, C, González-Dugo, V, Hernández, P, Sillero, JC, Zarco-Tejada, PJ (2018) Improved nitrogen retrievals with airborne-derived fluorescence and plant traits quantified from VNIR-SWIR hyperspectral imagery in the context of precision agriculture. *Int J Appl Earth Obs Geoinf* 70: 105–117. <https://doi.org/10.1016/j.jag.2018.04.013>

Chaerle, L, Lenk, S, Hagenbeek, D, Buschmann, C, Van Der Straeten, D (2007) Multicolor fluorescence imaging for early detection of the hypersensitive reaction to tobacco mosaic virus. *J Plant Physiol* 164(3): 253–262. <https://doi.org/10.1016/j.jplph.2006.01.011>

Chang, CY, Wen, J, Han, J, Kira, O, LeVonne, J, Melkonian, J, Riha, SJ, Skovira, J, Ng, S, Gu, L, Wood, JD, Nätke, P, Sun, Y (2021) Unpacking the drivers of diurnal dynamics of sun-induced chlorophyll fluorescence (SIF): Canopy structure, plant physiology, instrument configuration and retrieval methods. *Remote Sens Environ* 265: 112672. <https://doi.org/10.1016/j.rse.2021.112672>

Chaves, MM (1991) Effects of water deficits on carbon assimilation. *J Exp Bot* 42(1): 1–16. <https://doi.org/10.1093/jxb/42.1.1>

Chen, J M, Liu, J, Leblanc, SG, Lacaze, R, Roujean, JL (2003) Multi-angular optical remote sensing for assessing vegetation structure and carbon absorption. *Remote Sens Environ* 84(4): 516–525. [https://doi.org/10.1016/S0034-4257\(02\)00150-5](https://doi.org/10.1016/S0034-4257(02)00150-5)

Chen, X, Mo, X, Zhang, Y, Sun, Z, Liu, Y, Hu, S, Liu, S (2019) Drought detection and assessment with solar-induced chlorophyll fluorescence in summer maize growth period over North China Plain. *Ecol Indic* 104: 347–356. <https://doi.org/10.1016/j.ecolind.2019.05.017>

Chou, HM, Bundock, N, Rolfe, SA, Scholes, JD (2000) Infection of *Arabidopsis thaliana* leaves with *Albugo candida* (white blister rust) causes a reprogramming of host metabolism. *Mol Plant Pathol* 1(2): 99–113. <https://doi.org/10.1046/j.1364-3703.2000.00013.x>

Cordón, G. B., & Lagorio, M. G. (2006). Re-absorption of chlorophyll fluorescence in leaves revisited. A comparison of correction models. *Photoch Photobio Sci* 5: 735–740. <https://doi.org/10.1039/b517610g>

Cornic, G, Briantais, JM (1991) Partitioning of photosynthetic electron flow between CO₂ and O₂ reduction in a C₃ leaf (*Phaseolus vulgaris* L) at different CO₂ concentrations and during drought stress. *Planta* 183: 178–184. <https://doi.org/10.1007/BF00197786>

Cornic, G (2000) Drought stress inhibits photosynthesis by decreasing stomatal aperture—not by affecting ATP synthesis. *Trends Plant Sci* 5(5): 187–188. [https://doi.org/10.1016/S1360-1385\(00\)01625-3](https://doi.org/10.1016/S1360-1385(00)01625-3)

Curran, PJ (1989) Remote sensing of foliar chemistry. *Remote Sens Environ* 30(3): 271–278. [https://doi.org/10.1016/0034-4257\(89\)90069-2](https://doi.org/10.1016/0034-4257(89)90069-2)

D'Ambrosio, N, Arena, C, De Santo, AV (2006) Temperature response of photosynthesis, excitation energy dissipation and alternative electron sinks to carbon assimilation in *Beta vulgaris* L. *Environ Exp Bot* 55(3): 248–257. <https://doi.org/10.1016/j.envexpbot.2004.11.006>

Damm, A, Guanter, L, Paul-Limoges, E, Van der Tol, C, Hueni, A, Buchmann, N, Eugster, W, Ammann, C, Schaepman, ME (2015) Far-red sun-induced chlorophyll fluorescence shows ecosystem-specific relationships to gross primary production: An assessment based on observational and modeling approaches. *Remote Sens Environ* 166: 91–105. <https://doi.org/10.1016/j.rse.2015.06.004>

Dash, J, Curran, PJ (2004) The MERIS terrestrial chlorophyll index. *Int J Remote Sens* 25: 5403–5413. <https://doi.org/10.1080/0143116042000274015>

Datt, B (1998) Remote sensing of chlorophyll a, chlorophyll b, chlorophyll a+ b, and total carotenoid content in eucalyptus leaves. *Remote Sens Environ* 66(2): 111–121. [https://doi.org/10.1016/S0034-4257\(98\)00046-7](https://doi.org/10.1016/S0034-4257(98)00046-7)

De Cannière, S, Vereecken, H, Defourny, P, Jonard, F (2022) Remote sensing of instantaneous drought stress at canopy level using sun-induced chlorophyll fluorescence and canopy reflectance. *Remote Sens* 14(11): 2642. <https://doi.org/10.3390/rs14112642>

de Castro, AI, Shi, Y, Maja, JM, Peña, JM (2021) UAVs for vegetation monitoring: Overview and recent scientific contributions. *Remote Sens* 13(11): 2139. <https://doi.org/10.3390/rs13112139>

Dechant, B, Ryu, Y, Badgley, G, Zeng, Y, Berry, JA, Zhang, Y, Goulas, Y, Li, Z, Zhang, Q, Kang, M, Li, J, Moya, I (2020) Canopy structure explains the relationship between photosynthesis and sun-induced chlorophyll fluorescence in crops. *Remote Sens Environ* 241: 111733. <https://doi.org/10.1016/j.rse.2020.111733>

Demmig-Adams, B, Adams III, WW (2006) Photoprotection in an ecological context: The remarkable complexity of thermal energy dissipation. *New Phytol* 172(1): 11–21. <https://doi.org/10.1111/j.1469-8137.2006.01835.x>

Dey, PM, Harborne, JB (Eds) (1997) *Plant biochemistry*: 143–204. Elsevier. ISBN: 9780080525723

Evain, S, Flexas, J, Moya, I (2004) A new instrument for passive remote sensing: 2 Measurement of leaf and canopy reflectance changes at 531 nm and their relationship with photosynthesis and chlorophyll fluorescence. *Remote Sens Environ* 91(2): 175–185. <https://doi.org/10.1016/j.rse.2004.03.012>

Evans, JR (1989) Photosynthesis and nitrogen relationships in leaves of C3 plants. *Oecologia* 78: 9–19. <https://doi.org/10.1007/BF00377192>

Everaerts, J (2008) The use of unmanned aerial vehicles (UAVs) for remote sensing and mapping. *The International Archives of the Photogrammetry, Remote Sensing and Spatial Information Sciences* 37(2008): 1187–1192.

Farooq, S, Chmeliov, J, Wientjes, E, Koehorst, R, Bader, A, Valkunas, L, Trinkunas, G, van Amerongen, H (2018) Dynamic feedback of the photosystem II reaction centre on photoprotection in plants. *Nat Plants* 4(4): 225–231. <https://doi.org/10.1038/s41477-018-0127-8>

Farquhar, GD, von Caemmerer, SV, Berry, JA (1980) A biochemical model of photosynthetic CO₂ assimilation in leaves of C₃ species. *Planta* 149: 78–90. <https://doi.org/10.1007/BF00386231>

Féret, JB, François, C, Asner, GP, Gitelson, AA, Martin, RE, Bidel, LP, Ustin, SL, le Maire, G, Jacquemoud, S (2008) PROSPECT-4 and 5: Advances in the leaf optical properties model separating photosynthetic pigments. *Remote Sens Environ* 112(6): 3030–3043. <https://doi.org/10.1016/j.rse.2008.02.012>

Féret, JB, Berger, K, de Boissieu, F, Malenovský, Z (2021) PROSPECT-PRO for estimating content of nitrogen-containing leaf proteins and other carbon-based constituents. *Remote Sens Environ* 252: 112173. <https://doi.org/10.1016/j.rse.2020.112173>

Filella, I, Penuelas, J (1994) The red edge position and shape as indicators of plant chlorophyll content, biomass and hydric status. *Int J Remote Sens* 15(7): 1459–1470. <https://doi.org/10.1080/01431169408954177>

Filella, I, Porcar-Castell, A, Munné-Bosch, S, Bäck, J, Garbulsky, MF, Peñuelas, J (2009) PRI assessment of long-term changes in carotenoids/chlorophyll ratio and short-term changes in de-epoxidation state of the xanthophyll cycle. *Int J Remote Sens* 30(17): 4443–4455. <https://doi.org/10.1080/01431160802575661>

Flexas, J, Briantais, JM, Cerovic, Z, Medrano, H, Moya, I (2000) Steady-state and maximum chlorophyll fluorescence responses to water stress in grapevine leaves: a new remote sensing system. *Remote Sens Environ* 73(3): 283–297. [https://doi.org/10.1016/S0034-4257\(00\)00104-8](https://doi.org/10.1016/S0034-4257(00)00104-8)

Flexas, J, Bota, J, Escalona, JM, Sampol, B, Medrano, H (2002) Effects of drought on photosynthesis in grapevines under field conditions: an evaluation of stomatal and mesophyll limitations. *Funct Plant Biol* 29(4): 461–471. <https://doi.org/10.1071/PP01119>

Flexas, J, Bota, J, Loreto, F, Cornic, G, Sharkey, TD (2004) Diffusive and metabolic limitations to photosynthesis under drought and salinity in C₃ plants. *Plant Biol* 6(03): 269–279. <https://doi.org/10.1055/s-2004-820867>

Flexas, J, Diaz-Espejo, A, Galmes, J, Kaldenhoff, R, Medrano, H, Ribas-Carbo, M (2007) Rapid variations of mesophyll conductance in response to changes in CO₂ concentration around leaves. *Plant Cell Environ* 30(10): 1284–1298. <https://doi.org/10.1111/j.1365-3040.2007.01700.x>

Franck, F, Juneau, P, Popovic, R (2002) Resolution of the photosystem I and photosystem II contributions to chlorophyll fluorescence of intact leaves at room temperature. *BBA - Bioenergetics* 1556(2–3): 239–246. [https://doi.org/10.1016/S0005-2728\(02\)00366-3](https://doi.org/10.1016/S0005-2728(02)00366-3)

Frankenberg, C, Fisher, JB, Worden J, Badgley, G, Saatchi, SS, Lee, JE, Toon, GC, Butz, A, Jung, M, Kuze, A, Yokota, T (2011) New global observations of the terrestrial carbon cycle from GOSAT: Patterns of plant fluorescence with gross primary productivity. *Geophys Res Lett* 38(17). <https://doi.org/10.1029/2011GL048738>

Gamon, JA, Penuelas, J, Field, CB (1992) A narrow-waveband spectral index that tracks diurnal changes in photosynthetic efficiency. *Remote Sens Environ* 41(1): 35–44. [https://doi.org/10.1016/0034-4257\(92\)90059-S](https://doi.org/10.1016/0034-4257(92)90059-S)

Gamon, JA, Qiu, HL, Sanchez-Azofeifa, A (2007) Ecological applications of remote sensing at multiple scales. *Func Plant Ecol* (655–684) CRC Press.

Gamon, JA, Huemmrich, KF, Wong, CY, Ensminger, I, Garrity, S, Hollinger, DY, Noormets, A, Peñuelas, J (2016) A remotely sensed pigment index reveals photosynthetic phenology in evergreen conifers. *P Natl Acad Sci USA* 113(46): 13087–13092. <https://doi.org/10.1073/pnas.1606162113>

Garbulsky, MF, Peñuelas, J, Papale, D, Filella, I (2008) Remote estimation of carbon dioxide uptake by a Mediterranean forest. *Glob Change Biol* 14(12): 2860–2867. <https://doi.org/10.1111/j.1365-2486.2008.01684.x>

García-Plazaola, JI, Becerril, JM (2001) Seasonal changes in photosynthetic pigments and antioxidants in beech (*Fagus sylvatica*) in a Mediterranean climate: implications for tree decline diagnosis. *Funct Plant Biol* 28(3): 225–232. <https://doi.org/10.1071/PP00119>

Gastellu-Etchegorry, JP, Martin, E, Gascon, F (2004) DART: a 3D model for simulating satellite images and studying surface radiation budget. *Int J Remote Sens* 25(1): 73–96. <https://doi.org/10.1080/0143116031000115166>

Gates, DM (2012) *Biophysical ecology*: 490–526. Courier Corporation. ISBN: 0486428842

Genty, B, Briantais, JM, Baker, NR (1989) The relationship between the quantum yield of photosynthetic electron transport and quenching of chlorophyll fluorescence. *BBA-Gen Subjects* 990(1): 87–92. [https://doi.org/10.1016/S0304-4165\(89\)80016-9](https://doi.org/10.1016/S0304-4165(89)80016-9)

Gitelson, A, Merzlyak, MN (1994) Spectral reflectance changes associated with autumn senescence of *Aesculus hippocastanum* L and *Acer platanoides* L. leaves Spectral features and relation to chlorophyll estimation. *J Plant Physiol* 143(3): 286–292. [https://doi.org/10.1016/S0176-1617\(11\)81633-0](https://doi.org/10.1016/S0176-1617(11)81633-0)

Gitelson, A, Kaufman, YJ, Merzlyak, MN (1996) Use of a green channel in remote sensing of global vegetation from EOS-MODIS. *Remote Sens Environ* 58(3): 289–298. [https://doi.org/10.1016/S0034-4257\(96\)00072-7](https://doi.org/10.1016/S0034-4257(96)00072-7)

- Gitelson, AA, Buschmann, C, Lichtenthaler, HK (1998) Leaf chlorophyll fluorescence corrected for re-absorption by means of absorption and reflectance measurements. *J Plant Physiol* 152(2–3): 283–296. [https://doi.org/10.1016/S0176-1617\(98\)80143-0](https://doi.org/10.1016/S0176-1617(98)80143-0)
- Gitelson, A, Merzlyak, MN, Chivkunova, OB (2001) Optical properties and nondestructive estimation of anthocyanin content in plant leaves. *Photochem Photobiol* 74(1): 38–45. [https://doi.org/10.1562/0031-8655\(2001\)0740038OPANEO2.0.CO2](https://doi.org/10.1562/0031-8655(2001)0740038OPANEO2.0.CO2)
- Gitelson, A, Kaufman, YJ, Stark, R, Rundquist, D (2002) Novel algorithms for remote estimation of vegetation fraction. *Remote Sens Environ* 80(1): 76–87. [https://doi.org/10.1016/S0034-4257\(01\)00289-9](https://doi.org/10.1016/S0034-4257(01)00289-9)
- Gitelson, AA, Viña, A, Ciganda, V, Rundquist, DC, Arkebauer, TJ (2005) Remote estimation of canopy chlorophyll content in crops. *Geophys Res Lett* 32(8). <https://doi.org/10.1029/2005GL022688>
- Goerner, A, Reichstein, M, Tomelleri, E, Hanan, N, Rambal, S, Papale, D, Dragoni, D, Schmullius, C (2011) Remote sensing of ecosystem light use efficiency with MODIS-based PRI. *Biogeosciences* 8(1): 189–202. <https://doi.org/10.5194/bg-8-189-2011>
- Gu, L, Han, J, Wood, J D, Chang, CYY, Sun, Y (2019) Sun-induced Chl fluorescence and its importance for biophysical modeling of photosynthesis based on light reactions. *New Phytol* 223(3): 1179–1191. <https://doi.org/10.1111/nph.15796>
- Guanter, L, Alonso, L, Gómez-Chova, L, Amorós-López, J, Vila, J, Moreno, J (2007) Estimation of solar-induced vegetation fluorescence from space measurements. *Geophys Res Lett* 34(8). <https://doi.org/10.1029/2007GL029289>
- Guanter, L, Zhang, Y, Jung, M, Joiner, J, Voigt, M, Berry, JA, Frankenberg, C, Huete, AR, Zarco-Tejada, P, Lee, J-E, Moran, MS, Ponce-Campos, G, Beer, C, Camps-Valls, G, Buchmann, N, Gianelle, D, Klumpp, K, Cescatti, A, Baker, JM, Griffis, TJ (2014) Global and time-resolved monitoring of crop photosynthesis with chlorophyll fluorescence. *Proc Natl Acad Sci* 111(14). <https://doi.org/10.1073/pnas.1320008111>
- Gutman, G, Skakun, S, Gitelson, A (2021) Revisiting the use of red and near-infrared reflectances in vegetation studies and numerical climate models. *Sci Remote Sens* 4, 100025. <https://doi.org/10.1016/j.srs.2021.100025>
- Haboudane, D, Miller, JR, Pattey, E, Zarco-Tejada, PJ, Strachan, IB (2004) Hyperspectral vegetation indices and novel algorithms for predicting green LAI of crop canopies: Modeling and validation in the context of precision agriculture. *Remote Sens Environ* 90(3): 337–352. <https://doi.org/10.1016/j.rse.2003.12.013>
- Hamzeh, S, Naseri, AA, Alavipanah, SK, Mojaradi, B, Bartholomeus, HM, Clevers, JG, Behzad, M (2013) Estimating salinity stress in sugarcane fields with spaceborne hyperspectral vegetation indices. *Int J Appl Earth Obs* 21, 282–290. <https://doi.org/10.1016/j.jag.2012.07.002>

Hari, P, Keronen, P, Bäck, J, Altimir, N, Linkosalo, T, Pohja, T, Kulmala, M, Vesala, T (1999) An improvement of the method for calibrating measurements of photosynthetic CO₂ flux. *Plant Cell Environ* 22(10): 1297–1301. <https://doi.org/10.1046/j.1365-3040.1999.00478.x>

Hashmi, S, Younis, U, Danish, S, Munir, TM (2019) *Pongamia pinnata* L leaves biochar increased growth and pigments syntheses in *Pisum sativum* L. exposed to nutritional stress. *Agriculture - London* 9(7): 153. <https://doi.org/10.3390/agriculture9070153>

Hawkesford, M, Horst, W, Kichey, T, Lambers, H, Schjoerring, J, Møller, IS, White, P (2012) Functions of macronutrients. In *Marschner's mineral nutrition of higher plants*: 135–189. Academic press. <https://doi.org/10.1016/B978-0-12-384905-2.00006-6>

He, L, Magney, T, Dutta, D, Yin, Y, Köhler, P, Grossmann, K, Stutz, J, Dold, C, Hatfield, J, Guan, K, Peng, B, Frankenberg, C (2020) From the ground to space: Using solar-induced chlorophyll fluorescence to estimate crop productivity. *Geophys Res Lett* 47(7). <https://doi.org/10.1029/2020GL087474>

Heimann, M, Reichstein, M (2008) Terrestrial ecosystem carbon dynamics and climate feedbacks. *Nature* 451(7176): 289–292. <https://doi.org/10.1038/nature06591>

Helm, LT, Shi, H, Lerda, MT, Yang, X (2020) Solar-induced chlorophyll fluorescence and short-term photosynthetic response to drought. *Ecol Appl* 30(5). <https://doi.org/10.1002/eap.2101>

Hollinger, DY, Richardson, AD (2005) Uncertainty in eddy covariance measurements and its application to physiological models. *Tree Physiol* 25(7): 873–885. <https://doi.org/10.1093/treephys/25.7.873>

Horler, DNH, Dockray, M, Barber, J (1983) The red edge of plant leaf reflectance. *Int J Remote Sens* 4(2): 273–288. <https://doi.org/10.1080/01431168308948546>

Huang, D, Knyazikhin, Y, Dickinson, RE, Rautiainen, M, Stenberg, P, Disney, M, Lewis, P, Cescatti, A, Tian, Y, Verhoef, W, Martonchik, JV, Myneni, RB (2007) Canopy spectral invariants for remote sensing and model applications. *Remote Sens Environ* 106: 106–122. <https://doi.org/10.1016/j.rse.2006.08.001>

Huete, AR (1988) A soil-adjusted vegetation index (SAVI). *Remote Sens Environ* 25(3): 295–309. [https://doi.org/10.1016/0034-4257\(88\)90106-X](https://doi.org/10.1016/0034-4257(88)90106-X)

Huete, A, Didan, K, Miura, T, Rodriguez, EP, Gao, X, Ferreira, L G (2002) Overview of the radiometric and biophysical performance of the MODIS vegetation indices. *Remote Sens Environ* 83(1–2): 195–213. [https://doi.org/10.1016/S0034-4257\(02\)00096-2](https://doi.org/10.1016/S0034-4257(02)00096-2)

Ihuoma, SO, Madramootoo, CA (2019) Sensitivity of spectral vegetation indices for monitoring water stress in tomato plants. *Comput Electron Agr* 163, p104860. <https://doi.org/10.1016/j.compag.2019.104860>

- Jay, S, Maupas, F, Bendoula, R, Gorretta, N (2017) Retrieving LAI, chlorophyll and nitrogen contents in sugar beet crops from multi-angular optical remote sensing: Comparison of vegetation indices and PROSAIL inversion for field phenotyping. *Field Crop Res* 210: 33–46. <https://doi.org/10.1016/j.fcr.2017.05.005>
- Jia, J, Wang, Y, Chen, J, Guo, R, Shu, R, Wang, J (2020) Status and application of advanced airborne hyperspectral imaging technology: A review. *Infrared Phys Techn* 104, 103115. <https://doi.org/10.1016/j.infrared.2019.103115>
- Jia, M, Zhu, J, Ma, C, Alonso, L, Li, D, Cheng, T, Tian, Y, Zhu, Y, Yao, X, Cao, W (2018) Difference and potential of the upward and downward sun-induced chlorophyll fluorescence on detecting leaf nitrogen concentration in wheat. *Remote Sens* 10(8): 1315. <https://doi.org/10.3390/rs10081315>
- Jonasson, S (1988) Evaluation of the point intercept method for the estimation of plant biomass. *Oikos* 101–106. <https://doi.org/10.2307/3565988>
- Jordan, CF (1969) Derivation of leaf-area index from quality of light on the forest floor. *Ecology* 50(4): 663–666. <https://doi.org/10.2307/1936256>
- Kaiser, YI, Menegat, A, Gerhards, R (2013) Chlorophyll fluorescence imaging: a new method for rapid detection of herbicide resistance in *Alopecurus myosuroides*. *Weed Res* 53(6): 399–406. <https://doi.org/10.1111/wre.12043>
- Kanke, Y, Raun, W, Solie, J, Stone, M, Taylor, R (2012) Red edge as a potential index for detecting differences in plant nitrogen status in winter wheat. *J Plant Nutr* 35(10): 1526–1541. <https://doi.org/10.1080/01904167.2012.689912>
- Kitajima, M, Butler, WL (1975) Quenching of chlorophyll fluorescence and primary photochemistry in chloroplasts by dibromothymoquinone. *BBA - Bioenergetics* 376(1): 105–115. [https://doi.org/10.1016/0005-2728\(75\)90209-1](https://doi.org/10.1016/0005-2728(75)90209-1)
- Klughammer, C, Schreiber, U (1994) An improved method, using saturating light pulses, for the determination of photosystem I quantum yield via P700+-absorbance changes at 830 nm. *Planta* 192(2): 261–268. <https://doi.org/10.1007/BF00194461>
- Koh, JC, Banerjee, BP, Spangenberg, G, Kant, S (2022) Automated hyperspectral vegetation index derivation using a hyperparameter optimisation framework for high-throughput plant phenotyping. *New Phytol* 233(6): 2659–2670. <https://doi.org/10.1111/nph.17947>
- Kolari, P, Chan, T, Porcar-Castell, A, Bäck, J, Nikinmaa, E, Juurola, E (2014) Field and controlled environment measurements show strong seasonal acclimation in photosynthesis and respiration potential in boreal Scots pine. *Front Plant Sci* 5: 717. <https://doi.org/10.3389/fpls.2014.00717>
- Krall, JP, Edwards, GE (1992) Relationship between photosystem II activity and CO₂ fixation in leaves. *Physiol Plantarum* 86(1): 180–187. <https://doi.org/10.1111/j.1399-3054.1992.tb01328.x>

Kramer, DM, Johnson, G, Kiirats, O, Edwards, GE (2004) New fluorescence parameters for the determination of QA redox state and excitation energy fluxes. *Photosynth* 79(2): 209–218. <https://doi.org/10.1023/B:PRES.0000015391.99477.0d>

Lahlou, O, Ouattar, S, Ledent, JF (2003) The effect of drought and cultivar on growth parameters, yield and yield components of potato. *Agronomie* 23(3): 257–268. <https://doi.org/10.1051/agro:2002089>

Laisk, A, Loreto, F (1996) Determining photosynthetic parameters from leaf CO₂ exchange and chlorophyll fluorescence (ribulose-1, 5-bisphosphate carboxylase/oxygenase specificity factor, dark respiration in the light, excitation distribution between photosystems, alternative electron transport rate, and mesophyll diffusion resistance. *Plant Physiol* 110(3): 903–912. <https://doi.org/10.1104/pp.110.3.903>

Lambers, H; Oliveira, RS (2019) Plant Nutrient Use Efficiency. Mineral nutrition In *Plant Physiological Ecology* Springer: Berlin/Heidelberg, Germany: 301–384. <https://doi.org/10.1016/B978-0-12-819773-8.00007-1>

Larcher, W (2003) *Physiological plant ecology: ecophysiology and stress physiology of functional groups: 1-69.* Springer Science & Business Media. ISBN: 3540435166

Lassalle, G (2021) Monitoring natural and anthropogenic plant stressors by hyperspectral remote sensing: Recommendations and guidelines based on a meta-review. *Sci Total Environ* 788: 147758. <https://doi.org/10.1016/j.scitotenv.2021.147758>

Lazár, D (2015) Parameters of photosynthetic energy partitioning. *J Plant Physiol* 175: 131–147. <https://doi.org/10.1016/j.jplph.2014.10.021>

Li, F, Miao, Y, Feng, G, Yuan, F, Yue, S, Gao, X, Liu, Y, Liu, B, Ustin, SL, Chen, X (2014) Improving estimation of summer maize nitrogen status with red edge-based spectral vegetation indices. *Field Crop Res* 157: 111–123. <https://doi.org/10.1016/j.fcr.2013.12.018>

Li, Y, He, N, Hou, J, Xu, L, Liu, C, Zhang, J, Wang, Q, Zhang, X, Wu, X (2018) Factors Influencing Leaf Chlorophyll Content in Natural Forests at the Biome Scale. *Front Ecol Evol* 6. <https://doi.org/10.3389/fevo.2018.00064>

Liang, L, Di, L, Zhang, L, Deng, M, Qin, Z, Zhao, S, Lin, H (2015) Estimation of crop LAI using hyperspectral vegetation indices and a hybrid inversion method. *Remote Sens Environ* 165: 123–134. <https://doi.org/10.1016/j.rse.2015.04.032>

Lichtenthaler, HK, Rinderle, U (1988) The role of chlorophyll fluorescence in the detection of stress conditions in plants. *Crit Rev Anal Chem* 19: 29–85. <https://doi.org/10.1080/15476510.1988.10401466>

Liu, HQ, Huete, A (1995) A feedback based modification of the NDVI to minimize canopy background and atmospheric noise. *IEEE T Geosci Remote* 33(2): 457–465. <https://doi.org/10.1109/TGRS.1995.8746027>

Liu, W, Atherton, J, Möttus, M, Gastellu-Etchegorry, JP, Malenovský, Z, Raunonen, P, Åkerblom, M, Mäkipää, R, Porcar-Castell, A (2019) Simulating solar-induced chlorophyll fluorescence in a boreal forest stand reconstructed from terrestrial laser scanning measurements. *Remote Sens Environ* 232: 111274. <https://doi.org/10.1016/j.rse.2019.111274>

Lu, B, Dao, PD, Liu, J, He, Y, Shang, J (2020) Recent advances of hyperspectral imaging technology and applications in agriculture. *Remote Sens* 12(16): 2659. <https://doi.org/10.3390/rs12162659>

Lucht, W, Roujean, JL (2000) Considerations in the parametric modeling of BRDF and albedo from multiangular satellite sensor observations. *Remote Sens Rev* 18(2–4): 343–379. <https://doi.org/10.1080/02757250009532395>

Maas, SJ, Dunlap, JR (1989) Reflectance, transmittance, and absorptance of light by normal, etiolated, and albino corn leaves. *Agron J* 81(1): 105–110. <https://doi.org/10.2134/agronj1989.00021962008100010019x>

MacArthur, A, Robinson, I, Rossini, M, Davis, N, MacDonald, K (2014) A dual-field-of-view spectrometer system for reflectance and fluorescence measurements (Piccolo Doppio) and correction of etaloning. In *Fifth International Workshop on Remote Sensing of Vegetation Fluorescence* European Space Agency.

Magney, TS, Bowling, DR, Logan, BA, Grossmann, K, Stutz, J, Blanken, PD, Burns, SP, Cheng, R, Garcia, MA, Köhler, P, Lopez, S, Parazoo, NC, Raczka, B, Schimel, D, Frankenberg, C (2019) Mechanistic evidence for tracking the seasonality of photosynthesis with solar-induced fluorescence. *P Natl Acad Sci USA* 116(24): 11640–11645. <https://doi.org/10.1073/pnas.1900278116>

Magney, TS, Barnes, ML, Yang, X (2020) On the covariation of chlorophyll fluorescence and photosynthesis across scales. *Geophys Res Lett* 47(23). <https://doi.org/10.1029/2020GL091098>

Malenovský, Z, Mishra, KB, Zemek, F, Rascher, U, Nedbal, L (2009) Scientific and technical challenges in remote sensing of plant canopy reflectance and fluorescence. *J Exp Bot* 60(11): 2987–3004. <https://doi.org/10.1093/jxb/erp156>

Malenovský, Z, Lucieer, A, King, DH, Turnbull, JD, Robinson, SA (2017) Unmanned aircraft system advances health mapping of fragile polar vegetation. *Methods Ecol Evol* 8(12): 1842–1857. <https://doi.org/10.1111/2041-210X.12833>

Marceau, DJ, Hay, GJ (1999) Remote sensing contributions to the scale issue. *Can J Remote Sens* 25(4): 357–366. <https://doi.org/10.1080/07038992.1999.10874735>

Martini, D, Pacheco-Labrador, J, Perez-Priego, O, Van der Tol, C, El-Madany, T S, Julitta, T, Rossini, M, Reichstein, M, Christiansen, R, Rascher, U, Moreno, G, Pilar Martin, M, Yang, P, Carrara, A, Guan, J, González-Cascón, R, Migliavacca, M (2019) Nitrogen and

phosphorus effect on sun-induced fluorescence and gross primary productivity in mediterranean grassland. *Remote Sens* 11(21): 2562. <https://doi.org/10.3390/rs11212562>

Maxwell, K, Johnson, G N (2000) Chlorophyll fluorescence—a practical guide. *J Exp Bot* 51(345): 659–668. <https://doi.org/10.1093/jexbot/51.345.659>

McClain, AM, Sharkey, TD (2020) Building a better equation for electron transport estimated from Chl fluorescence: accounting for nonphotosynthetic light absorption. *New Phytol* 225(2): 604. <https://doi.org/10.1111/nph.16255>

McFarlane, JC, Watson, RD, Theisen, AF, Jackson, RD, Ehrlner, WL, Pinter, PJ, Idso, SB, Reginato, RJ (1980) Plant stress detection by remote measurement of fluorescence. *Appl Optics* 19(19): 3287–3289. <https://doi.org/10.1364/AO.19.003287>

Meroni, M, Colombo, R (2006) Leaf level detection of solar induced chlorophyll fluorescence by means of a subnanometer resolution spectroradiometer. *Remote Sens Environ* 103(4): 438–448. <https://doi.org/10.1016/j.rse.2006.03.016>

Meroni, M, Rossini, M, Guanter, L, Alonso, L, Rascher, U, Colombo, R, Moreno, J (2009) Remote sensing of solar-induced chlorophyll fluorescence: Review of methods and applications. *Remote Sens Environ* 113(10): 2037–2051. <https://doi.org/10.1016/j.rse.2009.05.003>

Merzlyak, MN, Chivkunova, OB, Solovchenko, AE, Naqvi, KR (2008) Light absorption by anthocyanins in juvenile, stressed, and senescing leaves. *J Exp Bot* 59(14): 3903–3911. <https://doi.org/10.1093/jxb/ern230>

Middleton, EM, Cheng, YB, Hilker, T, Black, TA, Krishnan, P, Coops, NC, Huemmrich, KF (2009) Linking foliage spectral responses to canopy-level ecosystem photosynthetic light-use efficiency at a Douglas-fir forest in Canada. *Can J Remote Sens* 35(2): 166–188. <https://doi.org/10.5589/m09-008>

Mohr, H, Schopfer, P (Eds) (2012) *Plant physiology: 1 – 6*. Springer Science & Business Media. <https://doi.org/10.1007/978-3-642-97570-7>

Monteith, JL (1972) Solar radiation and productivity in tropical ecosystems. *J Appl Ecol* 9(3): 747–766. <https://doi.org/10.2307/2401901>

Monteith, JL, Unsworth, MH, Webb, A (1994) Principles of environmental physics. *Q J Roy Meteor Soc* 120(520): 1699. <https://doi.org/10.1016/C2010-0-66393-0>

Montes, R, Ureña, C (2012) An overview of BRDF models. University of Grenada, Technical Report LSI–2012: 1, 19.

Morfopoulos, C, Sperlich, D, Peñuelas, J, Filella, I, Llusà, J, Medlyn, BE, Niinemets, Ü, Posell, M, Sun, Z, Prentice, IC (2014) A model of plant isoprene emission based on available reducing power captures responses to atmospheric CO₂. *New Phytol* 203(1): 125–139. <https://doi.org/10.1111/nph.12770>

- Munné-Bosch, S, Alegre, L (2004) Die and let live: leaf senescence contributes to plant survival under drought stress. *Funct Plant Biol* 31(3): 203–216. <https://doi.org/10.1071/FP03236>
- Myneni, RB, Hoffman, S, Knyazikhin, Y, Privette, JL, Glassy, J, Tian, Y, Wang, Y, Song, X, Zhang, Y, Smith, GR, Lotsch, A (2002) Global products of vegetation leaf area and fraction absorbed PAR from year one of MODIS data. *Remote Sens Environ* 83(1–2): 214–231. [https://doi.org/10.1016/S0034-4257\(02\)00074-3](https://doi.org/10.1016/S0034-4257(02)00074-3)
- Natr, L (1972) Influence of mineral nutrients on photosynthesis of higher plants. *Photosynthetica*, 6, 80–99.
- Nguy-Robertson, A, Gitelson, A, Peng, Y, Viña, A, Arkebauer, T, Rundquist, D (2012) Green leaf area index estimation in maize and soybean: Combining vegetation indices to achieve maximal sensitivity. *Agron J* 104(5): 1336–1347. <https://doi.org/10.2134/agronj2012.0065>
- Nigon, TJ, Mulla, DJ, Rosen, CJ, Cohen, Y, Alchanatis, V, Knight, J, Rud, R (2015) Hyperspectral aerial imagery for detecting nitrogen stress in two potato cultivars. *Comput Electron Agr* 112, 36–46. <https://doi.org/10.1016/j.compag.2014.12.018>
- Niinemets, U, Ellsworth, DS, Lukjanova, A, Tobias, M (2002) Dependence of needle architecture and chemical composition on canopy light availability in three North American *Pinus* species with contrasting needle length. *Tree Physiol* 22(11): 747–761. <https://doi.org/10.1093/treephys/22.11.747>
- North, PR (1996) Three-dimensional forest light interaction model using a Monte Carlo method. *IEEE T Geosci Remote* 34(4): 946–956. <https://doi.org/10.1109/36.508411>
- Obidiegwu, JE, Bryan, GJ, Jones, HG, Prashar, A (2015) Coping with drought: stress and adaptive responses in potato and perspectives for improvement. *Front Plant Sci* 6, 542. <https://doi.org/10.3389/fpls.2015.00542>
- Ögren, E (1988) Suboptimal nitrogen status sensitizes the photosynthetic apparatus in willow leaves to long term but not short term water stress. *Photosynth Res* 18, 263–275. <https://doi.org/10.1007/BF00034831>
- Olascoaga, B, Juurola, E, Pinho, P, Lukeš, P, Halonen, L, Nikinmaa, E, Bäck, J, Porcar-Castell, A (2014) Seasonal variation in the reflectance of photosynthetically active radiation from epicuticular waxes of Scots pine (*Pinus sylvestris*) needles. *Boreal Env Res* 19 (suppl B): 132–141.
- Pajares, G (2015) Overview and current status of remote sensing applications based on unmanned aerial vehicles (UAVs). *Photogramm Eng Rem S* 81(4): 281–330. <https://doi.org/10.14358/PERS.81.4.281>
- Panigada, C, Rossini, M, Meroni, M, Cilia, C, Busetto, L, Amaducci, S, Boschetti, M, Cogliati, S, Picchi, V, Pinto, F, Marchesi, A (2014) Fluorescence, PRI and canopy

temperature for water stress detection in cereal crops. *Int J Appl Earth Obs* 30, 167–178. <https://doi.org/10.1016/j.jag.2014.02.002>

Peng, Y, Gitelson, AA, Keydan, G, Rundquist, DC, Moses, W (2011) Remote estimation of gross primary production in maize and support for a new paradigm based on total crop chlorophyll content. *Remote Sens Environ* 115(4): 978–989. <https://doi.org/10.1016/j.rse.2010.12.001>

Peñuelas, J, Filella, I, Biel, C, Serrano, L, Save, R (1993) The reflectance at the 950–970 nm region as an indicator of plant water status. *Int J Remote Sens* 14(10): 1887–1905. <https://doi.org/10.1080/01431169308954010>

Peñuelas, J, Gamon, JA, Fredeen, AL, Merino, J, Field, CB (1994) Reflectance indices associated with physiological changes in nitrogen-and water-limited sunflower leaves. *Remote Sens Environ* 48(2): 135–146. [https://doi.org/10.1016/0034-4257\(94\)90136-8](https://doi.org/10.1016/0034-4257(94)90136-8)

Peñuelas, J, Filella, I (1998) Visible and near-infrared reflectance techniques for diagnosing plant physiological status. *Trends Plant Sci* 3(4): 151–156. [https://doi.org/10.1016/S1360-1385\(98\)01213-8](https://doi.org/10.1016/S1360-1385(98)01213-8)

Perera-Castro, AV, Flexas, J (2023) The ratio of electron transport to assimilation (ETR/AN): underutilized but essential for assessing both equipment's proper performance and plant status. *Planta* 257(2): 29. <https://doi.org/10.1007/s00425-022-04063-2>

Pérez-Priego, O, Zarco-Tejada, PJ, Miller, JR, Sepulcre-Cantó, G, Fereres, E (2005) Detection of water stress in orchard trees with a high-resolution spectrometer through chlorophyll fluorescence in-filling of the O2-A band. *IEEE T Geosci Remote* 43(12): 2860–2869. <https://doi.org/10.1109/TGRS.2005.857906>

Pfündel, E (1998) Estimating the contribution of photosystem I to total leaf chlorophyll fluorescence. *Photosynth Res* 56, 185–195. <https://doi.org/10.1023/A:1006032804606>

Pieruschka, R, Klimov, D, Kolber, ZS, Berry, JA (2010) Monitoring of cold and light stress impact on photosynthesis by using the laser induced fluorescence transient (LIFT) approach. *Funct Plant Biol* 37(5): 395–402. <https://doi.org/10.1071/FP09266>

Pisek, J, Ryu, Y, Alikas, K (2011) Estimating leaf inclination and G-function from leveled digital camera photography in broadleaf canopies. *Trees* 25, 919–924. <https://doi.org/10.1007/s00468-011-0566-6>

Porcar-Castell, A (2011) A high-resolution portrait of the annual dynamics of photochemical and non-photochemical quenching in needles of *Pinus sylvestris*. *Physiol Plant* 143(2): 139–153. <https://doi.org/10.1111/j.1399-3054.2011.01488.x>

Porcar-Castell, A, Garcia-Plazaola, JI, Nichol, CJ, Kolari, P, Olascoaga, B, Kuusinen, N, Fernández-Marin, B, Pulkkinen, M, Juurola, E, Nikinmaa, E (2012) Physiology of the seasonal relationship between the photochemical reflectance index and photosynthetic light use efficiency. *Oecologia* 170: 313–323. <https://doi.org/10.1007/s00442-012-2317-9>

Porcar-Castell, A, Tyystjärvi, E, Atherton, J, Van der Tol, C, Flexas, J, Pfündel, EE, Moreno, J, Frankenberg, C, Berry, JA (2014) Linking chlorophyll a fluorescence to photosynthesis for remote sensing applications: Mechanisms and challenges. *J Exp Bot* 65(15): 4065–4095. <https://doi.org/10.1093/jxb/eru191>

Porcar-Castell, A, Mac Arthur, A, Rossini, M, Eklundh, L, Pacheco-Labrador, J, Anderson, K, Balzarolo, M, Martín, MP, Jin, H, Tomelleri, E, Cerasoli, S, Sakowska, K, Hueni, A, Julitta, T, Nichol, CJ, Vescovo, L (2015) EUROSPEC: at the interface between remote-sensing and ecosystem CO₂ flux measurements in Europe. *Biogeosciences* 12: 6103–6124. <https://doi.org/10.5194/bg-12-6103-2015>

Porcar-Castell, A, Malenovsky, Z, Magney, T, Van Wittenberghe, S, Fernández-Marín, B, Maignan, F, Zhang, Y, Maseyk, K, Atherton, J, Albert, LP, Robson, TM, Zhao, F, Garcia-Plazaola, JI, Ensminger, I, Rajewicz, PA, Grebe, S, Tikkanen, M, Kellner, JR, Ihalainen, JA, Rascher U, Logan, B (2021) Chlorophyll a fluorescence illuminates a path connecting plant molecular biology to Earth-system science. *Nat Plants* 7(8): 998–1009. <https://doi.org/10.1038/s41477-021-00980-4>

Prasad, MNV (Ed) (1996) *Plant ecophysiology*: 3-40. John Wiley & Sons. ISBN: 0471131571

Quattrochi, DA, Goodchild, M F (Eds) (1997) *Scale in remote sensing and GIS*: 13-27. CRC press. ISBN: 156670104X

Rajewicz, PA, Zhang, C, Atherton, J, Van Wittenberghe, S, Riikonen, A, Magney, T, Fernandez-Marín, B, Gacia Plazaola, JI, Porcar-Castell, A (2023) The photosynthetic response of spectral chlorophyll fluorescence differs across species and light environments in a boreal forest ecosystem. *Agr Forest Meteorol* 334: 109434. <https://doi.org/10.1016/j.agrformet.2023.109434>

Rascher, U, Hütt, MT, Siebke, K, Osmond, B, Beck, F, Lüttge, U (2001) Spatiotemporal variation of metabolism in a plant circadian rhythm: the biological clock as an assembly of coupled individual oscillators. *P Natl Acad Sci USA* 98(20): 11801–11805. <https://doi.org/10.1073/pnas.191169598>

Rascher, U, Alonso, L, Burkart, A, Cilia, C, Cogliati, S, Colombo, R, Damm, A, Drusch, M, Guanter, L, Hanus, J, Hyvärinen, T, Julitta, T, Jussila, J, Kataja, K, Kokkalis, P, Kraft, S, Kraska, T, Matveeva, M, Moreno, J, Muller, O, Panigada, C, Pikel, M, Pinto, F, Prey, L, Pude, R, Rossini, M, Schickling, A, Schurr, U, Schüttemeyer, D, Verrelst, J, Zemek, F (2015) Sun-induced fluorescence—a new probe of photosynthesis: First maps from the imaging spectrometer HyPlant. *Glob Change Biol* 21(12): 4673–4684. <https://doi.org/10.1111/gcb.13017>

Reynolds-Henne, CE, Langenegger, A, Mani, J, Schenk, N, Zumsteg, A, Feller, U (2010) Interactions between temperature, drought and stomatal opening in legumes. *Environ Exp Bot* 68(1): 37–43. <https://doi.org/10.1016/j.envexpbot.2009.11.002>

Riihimäki, H, Luoto, M, Heiskanen, J (2019) Estimating fractional cover of tundra vegetation at multiple scales using unmanned aerial systems and optical satellite data. *Remote Sens Environ* 224, 119–132. <https://doi.org/10.1016/j.rse.2019.01.030>

Rolfe, SA, Scholes, JD (2010) Chlorophyll fluorescence imaging of plant–pathogen interactions. *Protoplasma* 247: 163–175. <https://doi.org/10.1007/s00709-010-0203-z>

Romero, JM, Cordon, GB, Lagorio, MG (2018) Modeling re-absorption of fluorescence from the leaf to the canopy level. *Remote Sens Environ* 204: 138–146. <https://doi.org/10.1016/j.rse.2017.10.035>

Rouse, JW, Haas, RH, Scheel, JA, Deering, DW (1974) Monitoring Vegetation Systems in the Great Plains with ERTS. *Proceedings, 3rd Earth Resource Technology Satellite (ERTS) Symposium 1*: 48–62.

Samanta, A, Das, G, Das, SK (2011) Roles of flavonoids in plants. *Carbon* 100(6): 12–35.

Satognon, F, Lelei, JJ, Owido, SF (2021) Use of GreenSeeker and CM-100 as manual tools for nitrogen management and yield prediction in irrigated potato (*Solanum tuberosum*) production. *Arch Agric Environ Sci* 6(2): 121–128. <https://dx.doi.org/10.26832/24566632.2021.060202>

Schreiber, U (2004) Pulse-amplitude-modulation (PAM) fluorometry and saturation pulse method: an overview. *Chlorophyll a fluorescence: a signature of photosynthesis*: 279–319. https://doi.org/10.1007/978-1-4020-3218-9_11

Sellers, PJ (1985) Canopy reflectance, photosynthesis and transpiration. *Int J Remote Sens* 6(8): 1335–1372. <https://doi.org/10.1080/01431168508948283>

Sellers, PJ, Schimel, DS, Moore III, B, Liu, J, Eldering, A (2018) Observing carbon cycle–climate feedbacks from space. *P Natl Acad Sci USA* 115(31): 7860–7868. <https://doi.org/10.1073/pnas.1716613115>

Shah, SH, Houborg, R, McCabe, MF (2017) Response of chlorophyll, carotenoid and SPAD-502 measurement to salinity and nutrient stress in wheat (*Triticum aestivum* L). *Agronomy* 7(3): 61. <https://doi.org/10.3390/agronomy7030061>

Shangguan, Z, Shao, M, Dyckmans, J (2000) Effects of nitrogen nutrition and water deficit on net photosynthetic rate and chlorophyll fluorescence in winter wheat. *J Plant Physiol* 156(1): 46–51. [https://doi.org/10.1016/S0176-1617\(00\)80271-0](https://doi.org/10.1016/S0176-1617(00)80271-0)

Sharp, R E, Matthews, M A, Boyer, J S (1984) Kok effect and the quantum yield of photosynthesis: light partially inhibits dark respiration. *Plant Physiol* 75(1): 95–101. <https://doi.org/10.1104/pp.75.1.95>

Sievänen, R, Godin, C, DeJong, TM, Nikinmaa, E (2014) Functional–structural plant models: a growing paradigm for plant studies. *Ann Bot - London* 114(4): 599–603. <https://doi.org/10.1093/aob/mcu175>

Silleos, NG, Alexandridis, TK, Gitas, IZ, Perakis, K (2006) Vegetation indices: advances made in biomass estimation and vegetation monitoring in the last 30 years. *Geocarto Int* 21(4): 21–28. <https://doi.org/10.1080/10106040608542399>

Song, L, Guanter, L, Guan, K, You, L, Huete, A, Ju, W, Zhang, Y (2018) Satellite sun-induced chlorophyll fluorescence detects early response of winter wheat to heat stress in the Indian Indo-Gangetic Plains. *Glob Change Biol* 24(9): 4023–4037. <https://doi.org/10.1111/gcb.14302>

Suárez, L, Zarco-Tejada, PJ, Berni, JAJ, González-Dugo, V, Fereres, E (2009) Modelling PRI for water stress detection using radiative transfer models. *Remote Sens Environ* 113(4): 730–744. <https://doi.org/10.1016/j.rse.2008.12.001>

Sun, Y, Frankenberg, C, Jung, M, Joiner, J, Guanter, L, Köhler, P, Magney, T (2018) Overview of solar-induced chlorophyll fluorescence (SIF) from the orbiting carbon Observatory-2: retrieval, cross-mission comparison, and global monitoring for GPP. *Remote Sens Environ* 209: 808–823. <https://doi.org/10.1016/j.rse.2018.02.016>

Sun, Y, Frankenberg, C, Wood, JD, Schimel, DS, Jung, M, Guanter, L, Drewry, DT, Verma, M, Porcar-Castell, A, Griffis, TJ, Gu, L (2017) OCO-2 advances photosynthesis observation from space via solar-induced chlorophyll fluorescence. *Science* 358(6360). <https://doi.org/10.1126/science.aam5747>

Sun, Y, Fu, R, Dickinson, R, Joiner, J, Frankenberg, C, Gu, L, Xia, Y, Fernando, N (2015) Drought onset mechanisms revealed by satellite solar-induced chlorophyll fluorescence: Insights from two contrasting extreme events. *J Geophys Res - Biogeo* 120(11): 2427–2440. <https://doi.org/10.1002/2015JG003150>

Sunil, B, Saini, D, Bapatla, RB, Aswani, V, Raghavendra, AS (2019) Photorespiration is complemented by cyclic electron flow and the alternative oxidase pathway to optimize photosynthesis and protect against abiotic stress. *Photosynth Res* 139: 67–79. <https://doi.org/10.1007/s11120-018-0577-x>

Swarbrick, PJ, Schulze-Lefert, P, Scholes, JD (2006) Metabolic consequences of susceptibility and resistance (race-specific and broad-spectrum) in barley leaves challenged with powdery mildew. *Plant Cell Environ* 29(6): 1061–1076. <https://doi.org/10.1111/j.1365-3040.2005.01472.x>

Taniguchi, M, LaRocca, C A, Bernat, J D, Lindsey, J S (2023) Digital database of absorption spectra of diverse flavonoids enables structural comparisons and quantitative evaluations. *J Nat Prod* 86(4): 1087–1119. <https://doi.org/10.1021/acs.jnatprod.2c00720>

Tetens, O (1930) Über einige meteorologische Begriffe. *Z geophys* 6: 297–309.

Theisen, AF (2002) Detecting chlorophyll fluorescence from orbit: the Fraunhofer line depth model. From laboratory spectroscopy to remotely sensed spectra of terrestrial ecosystems: 203–232 Dordrecht: Springer Netherlands.

Thomas, R (2008) Practical guide to ICP-MS: a tutorial for beginners. CRC press. <https://doi.org/10.1201/9781420067873>

Thomas, S, Kuska, M T, Bohnenkamp, D, Brugger, A, Alisaac, E, Wahabzada, M, et al (2018) Benefits of hyperspectral imaging for plant disease detection and plant protection: a technical perspective. *J Plant Dis Prot* 125: 5–20. <https://doi.org/10.1007/s41348-017-0124-6>

Tucker, C J (1979) Red and photographic infrared linear combinations for monitoring vegetation. *Remote Sens Environ* 8(2): 127–150. [https://doi.org/10.1016/0034-4257\(79\)90013-0](https://doi.org/10.1016/0034-4257(79)90013-0)

Tucker, CJ, Fung, IY, Keeling, CD, Gammon, RH (1986) Relationship between atmospheric CO₂ variations and a satellite-derived vegetation index. *Nature* 319(6050): 195–199. <https://doi.org/10.1038/319195a0>

Tyystjärvi, E (2013) Photoinhibition of photosystem II. *Int Rev Cel Mol Bio*: 300, 243–303. <https://doi.org/10.1016/B978-0-12-405210-9.00007-2>

Valladares, F, Pearcy, RW (1997) Interactions between water stress, sun-shade acclimation, heat tolerance and photoinhibition in the sclerophyll *Heteromeles arbutifolia*. *Plant Cell Environ*: 20(1): 25–36. <https://doi.org/10.1046/j.1365-3040.1997.d01-8.x>

Van Der Meer, F, Bakker, W, Scholte, K, Skidmore, A, De Jong, S, Clevers, JGPW, Addink, E, Epema, G (2001) Spatial scale variations in vegetation indices and above-ground biomass estimates: implications for MERIS. *Int J Remote Sens* 22(17): 3381–3396. <https://doi.org/10.1080/01431160152609227>

Van der Tol, C, Verhoef, W, Timmermans, J, Verhoef, A, Su, Z (2009) An integrated model of soil-canopy spectral radiances, photosynthesis, fluorescence, temperature and energy balance. *Biogeosciences* 6(12): 3109–3129. <https://doi.org/10.5194/bg-6-3109-2009>

Van der Tol, C, Berry, JA, Campbell, PKE, Rascher, U (2014) Models of fluorescence and photosynthesis for interpreting measurements of solar-induced chlorophyll fluorescence. *J Geophys Res - Biogeophys* 119(12): 2312–2327. <https://doi.org/10.1002/2014JG002713>

Verhoef, W (1998). Theory of radiative transfer models applied in optical remote sensing of vegetation canopies. Wageningen Agricultural University. ISBNL 90-5485-804-4

Verrelst, J, Rivera, JP, van der Tol, C, Magnani, F, Mohammed, G, Moreno, J (2015) Global sensitivity analysis of the SCOPE model: What drives simulated canopy-leaving sun-induced fluorescence? *Remote Sens Environ* 166: 8–21. <https://doi.org/10.1016/j.rse.2015.06.002>

Viña, A, Gitelson, AA (2005) New developments in the remote estimation of the fraction of absorbed photosynthetically active radiation in crops. *Geophys Res Lett* 32(17). <https://doi.org/10.1029/2005GL023647>

- Walker BJ, Kramer DM, Fisher N, Fu X (2020) Flexibility in the energy balancing network of photosynthesis enables safe operation under changing environmental conditions. *Plants* 9: 1–22. <https://doi.org/10.3390/plants9030301>
- Walter, A, Rascher, U, Osmond, B (2004) Transitions in photosynthetic parameters of midvein and interveinal regions of leaves and their importance during leaf growth and development. *Plant Biol* 6(02): 184–191. <https://doi.org/10.1055/s-2004-817828>
- Wang, Y, Suárez, L, Poblete, T, Gonzalez-Dugo, V, Ryu, D, Zarco-Tejada, PJ (2022) Evaluating the role of solar-induced fluorescence (SIF) and plant physiological traits for leaf nitrogen assessment in almond using airborne hyperspectral imagery. *Remote Sens Environ* 279: 113141. <https://doi.org/10.1016/j.rse.2022.113141>
- Wellburn, AR (1994) The spectral determination of chlorophylls a and b, as well as total carotenoids, using various solvents with spectrophotometers of different resolution. *J Plant Physiol* 144(3): 307–313. [https://doi.org/10.1016/S0176-1617\(11\)81192-2](https://doi.org/10.1016/S0176-1617(11)81192-2)
- Wu, H, Li, ZL (2009) Scale issues in remote sensing: A review on analysis, processing and modeling. *Sensors* 9(3): 1768–1793. <https://doi.org/10.3390/s90301768>
- Xu, S, Liu, Z, Zhao, L, Zhao, H, Ren, S (2018) Diurnal response of sun-induced fluorescence and PRI to water stress in maize using a near-surface remote sensing platform. *Remote Sens* 10(10): 1510. <https://doi.org/10.3390/rs10101510>
- Xu, S, Zaidan, M A, Honkavaara, E, Hakala, T, Viljanen, N, Porcar-Castell, A, Zhigang, L, Atherton, J (2020) On the estimation of the leaf angle distribution from drone based photogrammetry. *IEEE Int Geosci Remote Se*: 4379–4382. <https://doi.org/10.1109/IGARSS39084.2020.9323498>
- Xue, J, Su, B (2017) Significant remote sensing vegetation indices: A review of developments and applications. *J Sensors* 2017. <https://doi.org/10.1155/2017/1353691>
- Yang, J, Zhang, J, Wang, Z, Zhu, Q, Liu, L (2001) Water deficit–induced senescence and its relationship to the remobilization of pre-stored carbon in wheat during grain filling. *Agron J* 93(1): 196–206. <https://doi.org/10.2134/agronj2001.931196x>
- Yang, P, van der Tol, C (2018) Linking canopy scattering of far-red sun-induced chlorophyll fluorescence with reflectance. *Remote Sens Environ* 209: 456–467. <https://doi.org/10.1016/j.rse.2018.02.029>
- Yang, P, van der Tol, C, Campbell, PK, Middleton, EM (2021) Unraveling the physical and physiological basis for the solar-induced chlorophyll fluorescence and photosynthesis relationship using continuous leaf and canopy measurements of a corn crop. *Biogeosciences* 18(2): 441–465. <https://doi.org/10.5194/bg-18-441-2021>
- Yang, X, Tang, J, Mustard, JF, Lee, JE, Rossini, M, Joiner, J, Munger, W, Kornfeld, A, Richardson, AD (2015) Solar-induced chlorophyll fluorescence that correlates with canopy

photosynthesis on diurnal and seasonal scales in a temperate deciduous forest. *Geophys Res Lett* 42(8): 2977–2987. <https://doi.org/10.1002/2015GL063201>.

Ye, X, Abe, S, Zhang, S (2020) Estimation and mapping of nitrogen content in apple trees at leaf and canopy levels using hyperspectral imaging. *Precis Agric* 21: 198–225. <https://doi.org/10.1007/s11119-019-09661-x>

Yin, X, Lantiga, EA, Schapendonk, AH, Zhong, X (2003) Some quantitative relationships between leaf area index and canopy nitrogen content and distribution. *Ann Bot- London* 91(7): 893–903. <https://doi.org/10.1093/aob/mcg096>

Yin, X, Harbinson, J, Struik, PC (2009) A model of the generalized stoichiometry of electron transport limited C3 photosynthesis: Development and applications. *Photosynthesis in silico: understanding complexity from molecules to ecosystems*: 247–273. http://dx.doi.org/10.1007/978-1-4020-9237-4_11

Young, AJ (1991) The photoprotective role of carotenoids in higher plants. *Physiol Plantarum* 83(4): 702–708. <https://doi.org/10.1111/j.1399-3054.1991.tb02490.x>

Zarco-Tejada, PJ, Miller, JR, Mohammed, GH, Noland, TL, Sampson, PH (2002) Vegetation stress detection through chlorophyll a+ b estimation and fluorescence effects on hyperspectral imagery. *J Environ Qual* 31(5): 1433–1441. <https://doi.org/10.2134/jeq2002.1433>

Zarco-Tejada, PJ, González-Dugo, V, Berni, JA (2012) Fluorescence, temperature and narrow-band indices acquired from a UAV platform for water stress detection using a micro-hyperspectral imager and a thermal camera. *Remote Sens Environ* 117, 322–337. <https://doi.org/10.1016/j.rse.2011.10.007>

Zeng, Y, Badgley, G, Dechant, B, Ryu, Y, Chen, M, Berry, JA (2019) A practical approach for estimating the escape ratio of near-infrared solar-induced chlorophyll fluorescence. *Remote Sens Environ* 232: 111209. <https://doi.org/10.1016/j.rse.2019.05.028>

Zeng, Y, Hao, D, Park, T, Zhu, P, Huete, A, Myneni, R, Knyazikhin, Y, Qi, J, Nemani, RR, Li, F, Huang, J (2023) Structural complexity biases vegetation greenness measures. *Nat Ecol Evol* 1–9. <https://doi.org/10.1038/s41559-023-02187-6>

Zhang, C, Atherton, J, Peñuelas, J, Filella, I, Kolari, P, Aalto, J, Ruhanen, H, Bäck, J, Porcar-Castell, A (2019) Do all chlorophyll fluorescence emission wavelengths capture the spring recovery of photosynthesis in boreal evergreen foliage? *Plant Cell Environ* 42(12): 3264–3279. <https://doi.org/10.1111/pce.13620>

Zhang, C, Preece, C, Filella, I, Farré-Armengol, G, Peñuelas, J (2017) Assessment of the response of photosynthetic activity of Mediterranean evergreen oaks to enhanced drought stress and recovery by using PRI and R690/R630. *Forests* 8(10): 386. <https://doi.org/10.3390/f8100386>

Zhang, F, Zhou, G (2018) Research progress on monitoring vegetation water content by using hyperspectral remote sensing. *Chin J Plant Ecol* 42(5): 517–525. <https://doi.org/10.17521/cjpe.2017.0313>

Zhang, L, Shangguan, Z, Mao, M, Yu, G (2003) Effects of long-term application of nitrogen fertilizer on leaf chlorophyll fluorescence of upland winter wheat. *J Appl Ecol* 14(5): 695–698.

Zhang, Y, Guanter, L, Berry, JA, van der Tol, C, Yang, X, Tang, J, Zhang, F (2016) Model-based analysis of the relationship between sun-induced chlorophyll fluorescence and gross primary production for remote sensing applications. *Remote Sens Environ* 187: 145–155. <https://doi.org/10.1016/j.rse.2016.10.016>

Zhang, Z, Zhang, Y, Porcar-Castell, A, Joiner, J, Guanter, L, Yang, X, Migliavacca, M, Weimin, J, Zhigang, S, Shiping, C, Martini, D, Qian, Z, Zhaohui, L, Cleverly, J, Wang, H, Goulas, Y (2020) Reduction of structural impacts and distinction of photosynthetic pathways in a global estimation of GPP from space-borne solar-induced chlorophyll fluorescence. *Remote Sens Environ* 240: 111722. <https://doi.org/10.1016/j.rse.2020.111722>

Zou, X, Zhu, S, Möttus, M (2022) Estimation of canopy structure of field crops using sentinel-2 bands with vegetation indices and machine learning algorithms. *Remote Sens* 14(12). <https://doi.org/10.3390/rs14122849>